

**IMPACT OF AMORPHOUS SILICA SCALING ON THE STEAM PIPES
UTILIZATION IN THE OLKARIA GEOTHERMAL POWER PLANT
WELLS: A CASE OF WELL 37B IN THE OLKARIA EAST FIELD
PRODUCTION - NAIVASHA, KENYA**

BY

EKUAM PAUL ARONGAT

ENG/MES/12/19

A Thesis Submitted to the School of Engineering, Department of Mechanical,
Production and Energy Engineering in partial fulfillment for the requirements of the
award of the Degree of

MASTER OF SCIENCE

In

ENERGY STUDIES (*RENEWABLE ENERGY RESOURCES*)

MOI UNIVERSITY

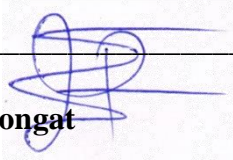
DECEMBER, 2022

DECLARATION

Declaration by candidate

This thesis is my original work which has never been presented to any university for an award of a degree. No part of this thesis may be reproduced manually, electronically or otherwise without prior permission of the author and/or Moi University.

Signature: _____



Date: 28th March 2022

Ekuam Paul Arongat

ENG/MES/12/19

Declaration by the supervisors

This thesis has been submitted for examination with our approval as the university supervisors.

Signature: _____



Date: 5th September, 2022

Prof. Zachary Otara Siagi,

Dept. of Mechanical, Production & Energy Engineering,
School of Engineering, Moi University

Signature: _____



Date: 5th September, 2022

Dr. Stephen Talai

Dept. of Mechanical, Production & Energy Engineering,
School of Engineering, Moi University

Signature: _____



Date: 5th September, 2022

Dr. Anthony Muliwa

Dept. of Chemical & Process Engineering,
School of Engineering, Moi University

DEDICATION

This work is dedicated to my parents, my late father Samson Arongat Engomo and my mother Selina Nasuru, for showing me the way of school at a young age, and to all those who may not be named here but who made significant contributions during my early schooling years.

ABSTRACT

Amorphous silica scaling in geothermal power plants has historically caused operational challenges such as obstructing fluid flow and reducing heat transfer efficiency, thus, limiting the overall power production. Similar problems are encountered in Kenya, and in particular Olkaria, therefore urgent attention is needed to mitigate this problem. This study therefore, aims at investigating sustainable ways of mitigating the effects caused by the amorphous silica scales deposition in the steam pipes in well 37B. The specific objectives were to determine the chemical composition of the brine, dry steam and steam condensate, perform chemical analysis on the scale deposits, evaluate parameters that influence scales formation in the steam pipes, and demonstrate the effect of scaling on plant power output. To achieve this, brine and steam samples were collected from the well using standard methods for sampling two-phase geothermal fluids and were chemically analyzed using titrimetric, spectroscopy and chromatography. Scale deposits were also collected from the separator U-seal, silencer, and turbine rotor for identification and structural characterization using X-ray diffraction (XRD) technique. The speciation computer code WATCH was used to evaluate processes that could influence the fluid composition and predictions for scale forming minerals. X-ray diffraction analysis revealed a broad diffraction peak at 23 angstrom on the 2D- θ scale indicating that the scale was mainly amorphous silica. The temperature of the brine was found to control the scaling conditions, with pro grade solubility (solubility that decreases as temperature and pressure decreases and vice versa, such as for silicates) simulated from 350°C to 110°C. It was noted that amorphous silica deposition occurs in fluids characterized by a wide range of total silica concentrations (350-700 ppm), temperature below 100°C, pH (4.5-5.5), and total dissolved solids concentrations (30-50 ppm). Consequently, temperature and pressure decrease was a significant cause of scaling while pH decrease was the principal cause of scaling. It was noted that the deposition of total dissolved solids, silica and other solutes contained in the dry steam carryover on the turbine reduces number of revolutions per second of the blades, hence lowering efficiency of the turbine blades rotation and, as a result, reducing the power output of the plant. Furthermore, in order to increase the pH, there was a need of reinjecting the diluted mixture of the steam condensates of a pH < 2.5 and temperature > 50°C from the power plants with the separated brine of a pH > 8.0 and temperature > 150°C into the wells, this was to increase the pH of the resultant mixture, and maintain temperature above the silica saturation temperature, thus, preventing deposition of the amorphous silica in the steam pipes. There was also a need to dispose of high temperature water (steam condensate) at temperatures above amorphous silica saturation (say above > 100°C for Olkaria wells), by reinjecting it back into the wells, thus preventing deposition of the scales in the steam pipes. The findings of this study revealed that pH decrease was the main cause of amorphous silica scales deposition while temperature and pressure decrease were responsible for scaling in the steam pipes.

TABLE OF CONTENTS

DECLARATION	ii
DEDICATION	iii
ABSTRACT	iv
TABLE OF CONTENTS	v
LIST OF TABLES	ix
LIST OF FIGURES	x
ACRONYMS	xi
ACKNOWLEDGEMENT	xii
CHAPTER ONE: INTRODUCTION	1
1.1 Background and Motivation	1
1.2 Statement of the Problem	6
1.3 Justification of the Study	6
1.4 Research Objectives	7
1.4.1 The main research objective	7
1.4.2 Specific objectives	7
1.5 Scope of the Study	8
1.6 Limitations of the Study	8
CHAPTER TWO: LITERATURE REVIEW	9
2.1 Introduction to geothermal fluids	9
2.2 Olkaria geothermal fluid characteristic	11
2.3 Olkaria East field production geothermal reservoir	14
2.3.1 Olkaria East field production ternary diagram Cl-SO ₄ -HCO ₃	15
2.4 Hypothetical background on scaling depositions	17
2.5 Conditions and mechanism of formation of silica scales	17

2.6 Geothermal scales formation and deposition.....	20
2.6.1 Factors affecting the formation of amorphous silica scaling	23
2.6.2 Methods of detecting solid deposits	23
2.6.3 How scale build-up impacts heat transfer	24
2.6.4 Silica scale deposition	25
2.6.5 Amorphous silica.....	27
2.7 Types of Scale.....	29
2.7.1 Calcium carbonate scales	29
2.7.2 Iron silicate scales	30
2.7.3 Sulphide scales	31
2.8 Methods for controlling scales deposition	31
2.8.1 X-ray diffraction (XRD) characterization of solid scales deposits	35
CHAPTER THREE: MATERIALS AND METHODS	37
3.1 Overview	37
3.2 Sampling Equipment.....	37
3.3 Sample Treatment and Preservation	38
3.4 Sampling Procedure	38
3.5 Chemical Analysis of the Brine and Steam Samples.....	41
3.5.1 Determination of pH.....	41
3.5.2 Determination of H ₂ S	42
3.5.3 Determination of CO ₂	42
3.5.4 Determination of conductivity and total dissolved solids (TDS)	42
3.5.5 Determination of high chloride > 20 ppm	43
3.5.6 Determination of high silica >20 ppm.....	43
3.5.7 Determination of low silica < 20 ppm.....	43

3.5.8 Determination of sulfates (SO_4^{2-})	44
3.5.9 Determination of Boron.....	44
3.5.10 Determination of low chloride < 20 ppm	44
3.5.11 Determination of fluoride ions	45
3.6 Sampling, analysis, and structural characterization of the scale deposit	46
CHAPTER FOUR: RESULTS AND DISCUSSION	48
4.1 Introduction.....	48
4.2 Physical and chemical composition of brine samples before steam extraction at the separator	49
4.3 Physical and chemical composition of steam samples at the turbine inlet	50
4.4 Chemical composition of steam condensate at the turbine exhaust.....	51
4.5 Structural characterization of scale deposits.....	52
4.5.1 XRF and XRD analysis report for the scale samples collected from the cyclone separator u-seal pit.....	53
4.5.2: XRF and XRD analysis report for scale samples collected from the silencer	55
4.5.3 XRF and XRD analysis report for scale samples collected from the turbine exhaust	57
4.6 Chemical analysis for the scaling potential	60
4.6.1 Overview of scale deposition	61
4.6.2 Deposition rate in Well 37B	65
4.6.3 The solubility of amorphous silica scales.....	65
4.6.4 The effect of temperature and pH on the deposition of amorphous silica scaling at well 37B.....	68
4.6.5 Effects of amorphous silica scaling on pressure drop	70

4.7 Effect of Amorphous Silica Scales Deposition on the Turbine and Plant Power	
Output	72
4.7.1 Decline of well 37B power output	72
4.7.2 Effects of amorphous silica scales on the turbine output	75
CHAPTER FIVE: CONCLUSIONS AND RECOMMENDATIONS	77
5.1 Conclusions.....	77
5.2 Recommendations.....	78
5.3 Contributions to new knowledge from this research work	80
REFERENCES.....	81
APPENDICES	86
Appendix A: Data for Brine and Scales Samples Analysis	86

LIST OF TABLES

Table 3.1: Standard methods use for the analysis of different elements in the collected samples (Arnorsson & Stefansson, 2012).....	46
Table 4.1: Brine sample analysis data before steam extraction at the separator.....	49
Table 4.2: Steam sample analysis data at the turbine inlet	50
Table 4.3: Chemical composition of the steam phase.....	51
Table 4.4: Steam condensate sample analysis at the turbine exhaust	51
Table 4.5: XRF analysis report for the scale deposits` samples	53
Table 4.6: XRD analysis report for scale deposits` samples	54
Table 4.7: XRF analysis report for the scale deposits` samples	55
Table 4.8: XRD analysis report for the scale deposits` samples.....	56
Table 4.9: XRF analysis report for the scale deposits` sample.....	58
Table 4.10: XRD analysis report for the scale deposits` sample	58
Table 4.11: Well 37B output between October 2019 and January 2020	61
Table 4.12: Thickness of the scale measurements taken at different positions of the steam pipeline	63
Table 4.13: Calculations of deposition rate in well 37B.....	65
Table 4.14: Wellhead pressure drop of well 37B after several months of production	73
Table 4.15: Effects of amorphous silica scales on the turbine output	75

LIST OF FIGURES

Figure 1.1: Shows sample of pipe with thickest silica scale deposit	3
Figure 1.2: Massive silica scales depositions at joints, elbows and valves	4
Figure 2.1: Geothermal fields within the greater Olkaria geothermal area	12
Figure 2.2: Olkaria East fluid classification	16
Figure 2.3: Turbine blades with silica deposits on nozzles from Olkaria II power plant	34
Figure 2.4: Steam valve with silica scales from Olkaria II power plant.....	35
Figure 3.1: Schematic diagrams of a two-phase pipeline that carries well discharges from the wellhead to an atmospheric silencer	39
Figure 3.2: Experimental set up of a Webre separator.....	40
Figure 4.1: % composition of scale deposit samples	53
Figure 4.2: Images of scale samples collected from the separator –u seal pit.....	55
Figure 4.3: % composition of scale deposit samples	56
Figure 4.4: An image of scale sample collected from the silencer	57
Figure 4.5: % composition of scale deposit samples	58
Figure 4.6: An image of scale sample collected from the turbine exhaust	60
Figure 4.7: XRD peaks for scale samples from the inside of the separator, silencer and from the turbine rotor.....	62
Figure 4.8: Thickness of scale deposited in two-phase fluid pipeline	63
Figure 4.9: Thickness of scale deposited in separated water pipeline	64
Figure 4.10: Thickness of scale at the T-Connection of well 37B.....	64
Figure 4.11: T-Connection on well 37B	64
Figure 4.12: Temperature dependence of the solubility of quartz and amorphous forms of silica.....	67
Figure 4.13: The estimated amorphous silica solubility with temperature in well 37B	68
Figure 4.14: The estimated amorphous silica solubility with pH	69

ACRONYMS

A.N.S.A	–	Amino Naphthalol Sulphonyl Acid
AAS	–	Atomic Absorption Spectrometer
GEA	–	Geothermal Energy Association
IC	–	Ion Chromatography
ICDD	–	International Centre for Diffraction Data
ICPS	–	Inductively Coupled Plasma Spectroscopy
KenGen	–	Kenya Electricity Generating Company
MoE	–	Ministry of Energy
MW	–	Megawatts
TCC	–	Total Carbonates Carbon
TDS	–	Total Dissolved Solids
UV / VL	–	Ultra violet / Visual light
XRD	–	X-Ray Diffraction

ACKNOWLEDGEMENT

I would like to thank the World Bank's ACE II PTRE initiative, which has helped me finance my studies and research. Without them, I would not have pursued a master's degree.

I want to express my gratitude to Moi University's School of Engineering for providing a welcoming learning environment for all students. I'm also grateful to my supervisors, Prof. Zachary Siagi, Dr. Stephen Talai, and Dr. Anthony Muliwa, for their unwavering support, guidance, time, advice, and motivation that helped to shape this thesis from the project proposal to the final draft; may God richly bless you.

I would also like to express my gratitude to the Electricity Generating Company (KenGen) for providing me with the opportunity to conduct research in the Olkaria Geothermal Fields. I would like to express my gratitude to all members of the geochemistry, power plant, and reservoir chemistry teams for sharing their expertise during the research period. My warmest regards go to Mr. Benedict Ouma, Mr. Mapesa Patrick, Mr. Martin Opiyo, and Mr. Samuel Githii. Thank you for your patience and for taking the time, considering your busy schedules, to walk me through the analytical procedures.

My heartfelt gratitude to my sisters, Esther Lobuin and Elizabeth Moru, who supported me financially during my studies, as well as my Children Julie Akiru, Liam Fadhili and Emmanuel Okoth who had to put up with my long absence. You were all very encouraging when I called and spoke with you. Thank you almighty God, for keeping me safe during my school years.

CHAPTER ONE

INTRODUCTION

1.1 Background and Motivation

Fossil fuels have long been the world's main sources of energy, accounting for over 80% of global primary energy consumption. Over time, there has been more understanding of the negative impacts of excessive fossil fuel burning on the environment due to greenhouse gas emissions (GHGs). As a result, there is increasing interest around the world in using renewable and environmentally friendly alternative energy sources. Nearly 1.6 billion people, or about a quarter of the global population, require modern energy services (Fridleifsson, 2011). However, recent events such as rising tensions in oil-rich countries and the resultant price volatility, growing energy regulations, environmental legislation, and limited resources, calls for a balanced energy mix and the most efficient use of available resources. This entails gaining a thorough understanding of energy resources, energy producing processes, and facilities, as well as developing detailed maintenance strategies to improve their performance and maximize resource use (World Energy Council, 2014).

In Kenya, electricity is generated using a variety of energy sources ranging from hydro, geothermal, thermal, biomass, solar, and wind. National power consumption by mode is currently 826.3 MW hydro, 828.04 MW geothermal, 2 MW biomass, 52 MW solar, 336.05 MW wind and 256 MW thermal (Ministry of Energy, 2018). It is evident that geothermal energy is one of the country's main energy sources. Exploration and infrastructure growth of geothermal power is being aggressively pursued with the global move towards clean, environmentally sustainable renewable energies. For example, geothermal energy has many advantages as geothermal energy appears as one

of the cleanest and most environmentally friendly sources compared to other energy sources such as coal, natural gas and even some renewable energy sources. Geothermal plants typically have small land footprints and low air pollution, geothermal power can also be generated as a renewable energy resource base load, which means that it operates 24 hours a day, 7 days a week, regardless of changing weather, providing a special, stable and continuous source of clean energy, and ultimately geothermal power generates employment and stimulates economic growth often in rural areas with high unemployment rates (Ministry of Energy, 2018).

Geothermal energy is energy contained in intense heat which flows outward continuously from deep within the crust of the earth. This heat mainly originates in the core. The crust, the outer layer of the earth, and the decay of radioactive elements that are in all rocks produce some heat. In the form of fumaroles, hot springs and hot altered energy is manifested on the earth's surface. Wells are drilled at depths of 1-3 km to tap steam and water at high temperatures (250-350°C) and pressures (600-1200 psi) to extract this energy. The dry steam is extracted from the brine at the separator for electricity generation, and used to drive a turbine coupled to a generator to generate electricity. There is almost no emission of such environmental contaminants so there is no need to burn fuels like oil, coal and natural gas. Geothermal energy is renewable energy that is reusable and its use is expected to increase in the future to help prevent global warming. However, geothermal steam often contains large amounts of minerals and gases in various quantities, depending on the geological structure and hydrological status of the earth's crust, resulting in its thermodynamic properties being affected. These impurities often lead to numerous defects in wells and surface installations within which geothermal fluids flow, such as scaling or solid deposition (KenGen, 2011).

Scales are heavy coatings that occur as a result of super saturation of soluble minerals of primarily inorganic materials. It occurs as a result of geothermal water contact with rocks and deep boiling processes in the reservoir, resulting in supersaturated water due to mineral dissolution. Dissolution may be accelerated by temperature and sometimes it may deteriorate depending on the solute (Gunnarsson, Arnorsson, & Jakobsson, 2015). Scaling of steam pipes caused by silica deposition is a worldwide issue in the geothermal industry and its primary effect is to limit the development of geothermal resources for the generation of electricity. Cleaning steam pipes and injection wells is costly undertaking, which generally raises power plant maintenance and operating costs, which has a direct impact on plant profitability.



Figure 1.1: Shows sample of pipe with thickest silica scale deposit
(Source: KenGen geochemistry laboratory, 2014)



Figure 1.2: Massive silica scales depositions at joints, elbows and valves
(Source: KenGen geochemistry laboratory, 2014)

Different types of geothermal fluids from different wells produce brine with varying chemical conditions, which can be found in different parts of the world. Even within a single field's wells, significant variances can be discovered. The chemistry of these various brines differs, and the differences are dependent on a variety of factors such as the geology of the resource, temperature, pressure, and water source. Steam and water ratios in brine can vary significantly depending on the resource. The scaling properties of brine and steam pose a challenge in geothermal operations (Gunnarsson, Arnorsson, & Jakobsson, 2015).

For several decades, large-scale geothermal exploitation has been on-going in Kenya. The Olkaria power plant's first unit in Kenya was commissioned in 1986 and the second phase was commissioned in 2010. In recent years, the technology used to harness geothermal energy has improved a lot and steps have been taken to reduce the environmental impact of the use of geothermal energy, particularly by re-injecting used fluid into wells and direct drilling. Avoiding geothermal brine re-injection can result in a faster deterioration of reservoir pressure, which can therefore have a negative effect on the capacity of production wells. In the use of high-temperature geothermal fluids

for power generation, the key operational difficulties faced include the creation of different kinds of scales in production wells, surface equipment and injection wells. In the use of geothermal energy, the main problems emerge from the precipitation of solid scales from geothermal fluids. The scales trigger flow restrictions in certain situations, such as in boreholes, two-phase pipelines, separators and steam pipes. Scale formation also makes it difficult to close and open valves leading to leaks and also to deposit scales on turbine blades, resulting in a rise in turbine chest pressure (Corsi, 2011). Scaling in surface equipment typically results in the loss of capacity throughout the process for the steam pipes. In turn, this will reduce the geothermal plant's production. In addition, a shutdown might be necessary to clear the lines and equipment if the scaling is huge to allow the facility to operate at full capacity. If scaling is done on a regular basis, maintenance costs are increased and plant productivity is decreased (Villasenor, 2011).

In hydrothermal areas, silica deposition occurs in several forms at various depths. These include quartz, cristobalite, chalcedony, and amorphous silica. Of these, the most stable type of silica is quartz and has the lowest solubility. Deep geothermal water is normally quartz-stable at the underlying reservoir temperature. Due to the slow rate of formation, deposition of quartz in wellbores and surface equipment is not a common issue (Tassew, 2001). Amorphous silica is however associated with changes in temperature of the geothermal water. This is where the extraction of steam and cooling of fluids takes place. In surface equipment such as pipelines, separators, turbine nozzles, heat exchangers and re-injection wells, the deposition of amorphous silica from supersaturated water is the most alarming scale when precipitated. In geothermal fields with high heat content, this problem is more severe as steam separation takes place.

Silica scale deposition from geothermal fluids may occur after super saturation occurs over periods of minutes or hours. This is why silica deposition has been observed in many geothermal facilities in the fluid-handling equipment (Villasenor, 2011).

1.2 Statement of the Problem

In geothermal power fields, silica scaling is a primary challenge and measures have to be put in place to reduce its impact on the power plant during generation due to this problem. The type of scaling that occurs in the equipment of the power plants depends solely on the geology of the steam field formation. Mineral scaling will result in the diameter of the steam pipes being decreased, which increases the pumping power needed for the pipes to transfer water. Scaling also increases the thermal resistance of the steam pipes, causing it to take more heat to boil water or more cooling to reduce water temperatures and also restricts fluid flow inside the decreasing plant efficiency of the steam field equipment due to increased energy costs and when scaling is repeatedly encountered, a shutdown may be required to clear the lines, thereby reducing plant capacity. This study has therefore been developed for the purpose of mitigating scaling impact on the steam pipes in the Olkaria power station due to the mineral deposition of a type of amorphous silica. It is tiresome and expensive to overhaul and physically extract silica from the affected auxiliary components and that is why this study aims to examine the root cause of scaling deposition in the steam pipes such that proper solutions are found and implemented to minimize operational costs and increase the performance of the power plant.

1.3 Justification of the Study

Mineral scaling is one of the common challenges facing geothermal power production at Kenya's Olkaria power stations. These modifications contribute to the deposition of

dissolved minerals as highly mineralized geothermal fluids are extracted and subjected to changes in temperature and pressure, creating scaling problems for pipelines and power plant equipment. In general, the scaling of the surface facility would result in the loss of capacity of the steam pipes and, in turn, the performance of the geothermal plant will be decreased. In addition, if the scaling is large, a shutdown might be necessary to clear the lines and equipment to allow maximum capacity operation of the facility and if scaling is often encountered, it raises maintenance costs. As the geothermal fluid flows from the production well, this fluid composition varies from solid particles to chemical compounds, all of which could impact the operation and the equipment. Therefore, there is a need to understand the root cause of the scaling or deposition of silica on steam pipes in order to evaluate and incorporate suitable solutions to increase the performance of the plant and minimize operating costs.

1.4 Research Objectives

1.4.1 The main research objective

To investigate sustainable ways of mitigating problems caused by the impact of amorphous silica scaling on the steam pipes in the Olkaria geothermal power plant wells in Naivasha, Kenya.

1.4.2 Specific objectives

The specific objectives for the study were:

- i. To determine the chemical composition of the brine, dry steam and steam condensate of well 37B in Olkaria East production field.

- ii. To perform physico-chemical analysis on the scale deposits samples collected inside the two-phase fluid pipeline.
- iii. To identify parameters that influence scales formation in the steam pipes and plant equipment's of well 37B.
- iv. To establish the effect of amorphous silica scaling deposition on plant power output.

1.5 Scope of the Study

This study was confined to the following areas;

- i. This research was limited to Olkaria geothermal East field. It is one of the seven fields of the greater Olkaria geothermal area.
- ii. Sampling of geothermal fluids was carried out at three different locations i.e. collection of the brine at the wellhead before steam extraction at the separator, dry steam at the turbine inlet, and steam condensate at the turbine exhaust.
- iii. Chemical analysis of the brine and steam samples
- iv. Sampling, analysis and characterization of the scale deposits

1.6 Limitations of the Study

Results analysis of the steam, brine and scales from this field may differ from other geothermal fields.

CHAPTER TWO

LITERATURE REVIEW

2.1 Introduction to geothermal fluids

Geothermal fluids refer to the liquid, steam and gas of geothermal energy. The state in which the fluid is in either liquid or vapor depends on the pressure and temperature. It is referred to as a two-phase flow when the fluid travels as a combination of fluid and vapor, i.e. gas and steam. The dissolved minerals are practically only present in the liquid phase, such as silica and salts. Another geothermal fluid portion is gas that is dissolved in the liquid phase, primarily carbon dioxide, hydrogen sulphide, hydrogen, nitrogen and methane. These gases are easily moved to the steam process immediately boiling starts, as the gas molecules tend to live in steam instead of water. The dissolved CO₂ and H₂S gases are weak acids and once boiling starts the acid gases exit the liquid phase to the steam phase and the liquid becomes more basic with a higher pH (Villasenor, 2011).

Geothermal fluid chemistry depends on the type of geothermal reservoir, so the geothermal fluid composition varies from one geothermal reservoir to the other, and can differ within the same geothermal reservoir as well. These differences are due to temperature, gas content, heat source, type of rock, rock permeability, hydrothermal system age, and fluid source age variations (Barbier, 2012).

Geothermal fluid encompasses geothermal liquid, steam, and gas, either alone or in combination. The pressure and temperature determine whether the fluid is in the state of liquid or vapour. Two-phase flow describes when a fluid travels as a mixture of liquid and vapor, such as gas and steam. Silica and salts, which are dissolved minerals, can only be found in liquid form. Gases, primarily carbon dioxide, are also present in

geothermal fluids and are dissolved in the liquid phase until the water boils. H₂S, hydrogen, nitrogen, and methane are some of the other gases. Because gas molecules prefer to be in the steam phase, the gases are quickly transferred to it as they boil (Thorhallsson, 2012).

Different concentrations of dissolved minerals and gases are carried by geothermal fluids. Geochemists are experts in this field, having discovered over twenty chemical species and chemical ratios that are influenced by temperature. Geothermometers are temperature indicators that are a vital tool in exploration because chemical analysis of fluids alone can predict reservoir temperature and deduce a plethora of other valuable information about what is going on in the reservoir. Because the geothermal fluid has been in the reservoir for a long time and has thus established equilibrium with the minerals in the reservoir rock, this is the case (Thorhallsson, 2012).

Because most minerals, such as silica, are more soluble in hot water than in cold water, knowing the silica content in the water can tell us what the reservoir temperature is or has been. Because the fluid is saturated at reservoir temperature, any cooling will create super-saturation, resulting in the excess concentration precipitating. Mineral deposits generated in this manner are known to attach to pipes and other surfaces. Some minerals, like as calcite and calcium sulfate, are less soluble in water at higher temperatures, which is an advantage because it reduces the formation of such deposits when the fluid is utilized and cools down. Changes in the pH value have a similar impact on the chemical evolution of geothermal fluids as temperature and pressure do. This is due to the weak acidity of dissolved carbon dioxide and hydrogen sulphide gases. When boiling begins, acid gases leave the liquid and enter the steam phase, causing the liquid to become more basic, resulting in a higher pH. The overall effect of

cooling and steam separation is highly complex, and computer chemical modeling is required to keep track of the changes that occur (Thorhallsson, 2012).

The solubility product for specific minerals can be determined using information on chemical activity and concentrations of chemical species to evaluate if the fluid is supersaturated with regard to particular minerals and thus likely to form scale. These calculations all presume equilibrium to be attained, and while this occurs quickly for many minerals, some minerals take longer to equilibrate. Slow rates can occasionally be exploited by forcing the fluid to flow quickly through the device. As a result, knowing the rate of the precipitation reaction is critical for fluid handling system design. To influence the rate of silica precipitation, for example, changing the pH of the fluid by adding acid or caustic is used. The precipitation of a highly supersaturated solution is slowed when acid is added. If you want to extract silica from an acidified, extremely supersaturated solution, you can add caustic, which will promote fast precipitation.

2.2 Olkaria geothermal fluid characteristic

Commentate lavas and their pyroclastic counterparts, ashes from Suswa and Longonot volcanoes, and small trachyte and basalts make up the geology of the greater Olkaria volcanic complex and its surface outcrops. The presence of basalt (Olkaria basalt) underneath the upper Olkaria volcanoes in the Eastern part of the geothermal field is suggested by well lithological logs. The Olkaria geothermal field's subsurface geology has been divided into six lithostratigraphic classes based on age, tectono-stratigraphy, and lithology. The proterozoic "basement" formations, pre-Mau volcanos, Mau Tuffs, Plateau Trachyte, Olkaria Basalts, and Upper Olkaria Volcanos are among the formations in chronological order from oldest to youngest (Omenda, 2010).

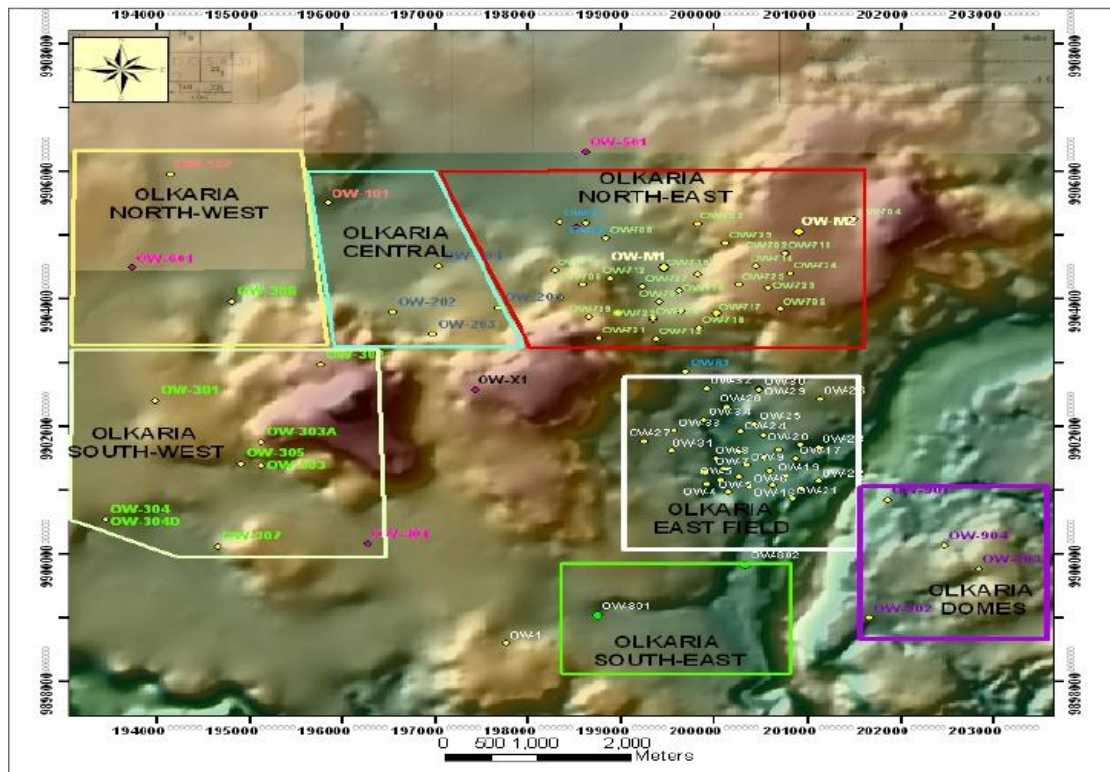


Figure 2.1: Geothermal fields within the greater Olkaria geothermal area
(Source: KenGen geothermal fields map, 2014)

The Olkaria fault, Gorge Farm faults, Suswa lineament, and Ol'Njorowa Gorge are among the structures contained in the greater Olkaria volcanic complex. The faults are visible in the Olkaria Central and Olkaria West fields, but not in the Olkaria Domes region, probably due to the thick pyroclastic cover. The oldest faults are the NW-SE and WNW-ESE faults, which are connected to the formation of the main Rift Valley (Opondo, 2010). Although a single phase occurs to the north of the Olkaria fault zone, the Olkaria geothermal system is characterized by a liquid-dominated reservoir. When the first deep wells were drilled in the Olkaria East field, a two-phase reservoir overlain by a vapor-dominated (steam) cap existed above the liquid reservoir (Karingithi, 2010). Except for samples from Olkaria West, which tend to spread along the H_2O-CO_2 axis, reservoir fluids from Olkaria show the highest H_2O/CO_2 ratio. Strong H_2O/CO_2 ratios, on the other hand, tend to represent lower temperature fluids tapped from the shallower

aquifers in the wells. This hypothesis is based on the fact that most wells discharging two-phase fluids have different solute temperatures specifically silica temperatures (Malimo, 2013).

The content of N₂ in Olkaria fluid samples tended to be significantly enriched. Preferential nitrogen loss during boiling could explain differences in N₂ content, especially in wells with high heat flow and content. It's also possible that air contamination occurred during sampling and/or due to the presence of drilling fluids in the reservoir, which could explain the N₂ - rich samples, particularly for the wells that have been subjected to discharge testing up until now. In geothermal fluids, however, there are other sources of N₂. Analysis of well discharges has shown that wells have N₂ and Ar concentrations up to ten times higher than air saturated water (ASW) and concentrations as low as one tenth of ASW. Furthermore, experiments in Iceland have indicated that N₂ comes from a source other than air-saturated water, potentially entrapped air bubbles, magmatic gas, or rotting organic matter, based on N₂/Ar ratios (Giroud, 2012).

In contrast to Menengai, Olkaria wells tend to be depleted in H₂. Fluids from Menengai well MW-13 are the richest in H₂, with CO₂/H₂ ratios of less than 6, whereas fluids from wells MW-03 and MW-01 are the poorest in H₂, with CO₂/H₂ ratios of more than 30 and 70, respectively. The majority of Olkaria well fluids, as well as the fluids from wells MW-04, MW-06, MW-09, MW-19, MW-12, and MW-20, have intermediate properties, with $6 < \text{CO}_2 / \text{H}_2 < 30$. High H₂ concentrations in the aquifer liquid are typically interpreted as suggesting the presence of vapor fraction in the initial reservoir fluid, which increases the sparingly water soluble H₂ concentrations but not the more soluble CO₂ and H₂S concentrations (Arn`orsson, 2010).

As a result, the Menengai reservoir has a higher vapor fraction than the Olkaria reservoir. The concentrations of CH₄ differ, with the majority of samples ranging between 40 and 1200 units of CO₂/CH₄. The presence of different redox conditions, temperature, pressure, and vapor/(vapor + liquid) mass ratio (referred to as y value) in the zones where gas equilibration is attained could explain variations in H₂ and CH₄ contents from field to field and well to well. Since H₂ and CH₄ are minor components, chemical reactions are expected to affect them, particularly hydrogen, which is highly reactive, rather than methane, which is a “slow” species, especially at low temperatures.

The concentrations of reactive gases H₂S and H₂ in the Olkaria reservoir fluids are typically preserved in local equilibrium with the pyrite-pyrhotite-magnetite mineral assemblage, according to studies. Furthermore, in most parts of the geothermal region, CO₂ concentration is controlled by a near approach to local equilibrium with the Epidote-prehnite-calcite-quartz mineral assemblage, except in Domes and Olkaria West, where it is controlled by flux from the magma heat source. Furthermore, it was discovered that the mineral assemblage pyrite-pyrrhotite-magnetite regulates the concentrations of H₂S and H₂ in aquifer water (Karingithi, 2010).

2.3 Olkaria East field production geothermal reservoir

This reservoir produces two-phase mixture of steam and water in general proportion of 85% steam and 15% water, making it ideal for electrical power generation. The geothermal reservoir is a liquid-dominated high-temperature type, with an average down-hole temperature between 230 °C and 260 °C (Wambugu, 2011). Magmatic intrusions situated at depths of about 5 to 8 km represent the heat source of the device. High chloride-bicarbonate waters with low pH and high gas content show fluid chemistry of 0.75 percent in steam by weight.

Deep in the well, boiling begins and the two-phase flow passes tangentially from the well through the pipeline to cyclone separators for separation at a pressure of about 6 bars. As brine is pumped into 4 hot re-injection wells, the separated steam step passes through the steam pipeline network to the power station. The long water column is extracted by blowing it into a wellhead silencer after a long well shut-in, water then moves to a holding pod via an open channel until it is pumped to two cold-injection wells outside the production area. The well is then linked to the station with a steam pipeline.

2.3.1 Olkaria East field production ternary diagram Cl-SO₄-HCO₃

The classification of thermal water is based on the relative concentrations of the three major anions Cl⁻, SO₄²⁻ and HCO₃⁻ according to (Giggenbach W. F., 2012). After dissolving, chloride, which is a conservative ion in geothermal fluids, does not engage in reactions with rocks. After it has dissolved, chloride does not precipitate; its concentration is independent of the mineral equilibria that regulate the concentrations of the constituents forming the rock. Therefore, in geothermal studies, chloride is used as a tracer. One diagram for the classification of natural waters is the Cl-SO₄-HCO₃ ternary diagram (Giggenbach W. F., 2012). Several forms of thermal water can be differentiated by using it i.e. mature waters, peripheral waters, volcanic waters, and steam-heated waters. An initial indication of blending relationships is given in the diagram. The chloride-rich waters are normally located near the upstream flow zones of geothermal systems according to (Giggenbach W. F., 2012). In the more elevated sections of a sector, high SO₄²⁻ steam-heated waters are typically found. The degree of separation between the high chloride and bicarbonate water data points would show the relative degree of contact between the lower temperatures of the carbon dioxide charged

fluid and the bicarbonate ion concentrations that increase with the time and distance travelled underground.

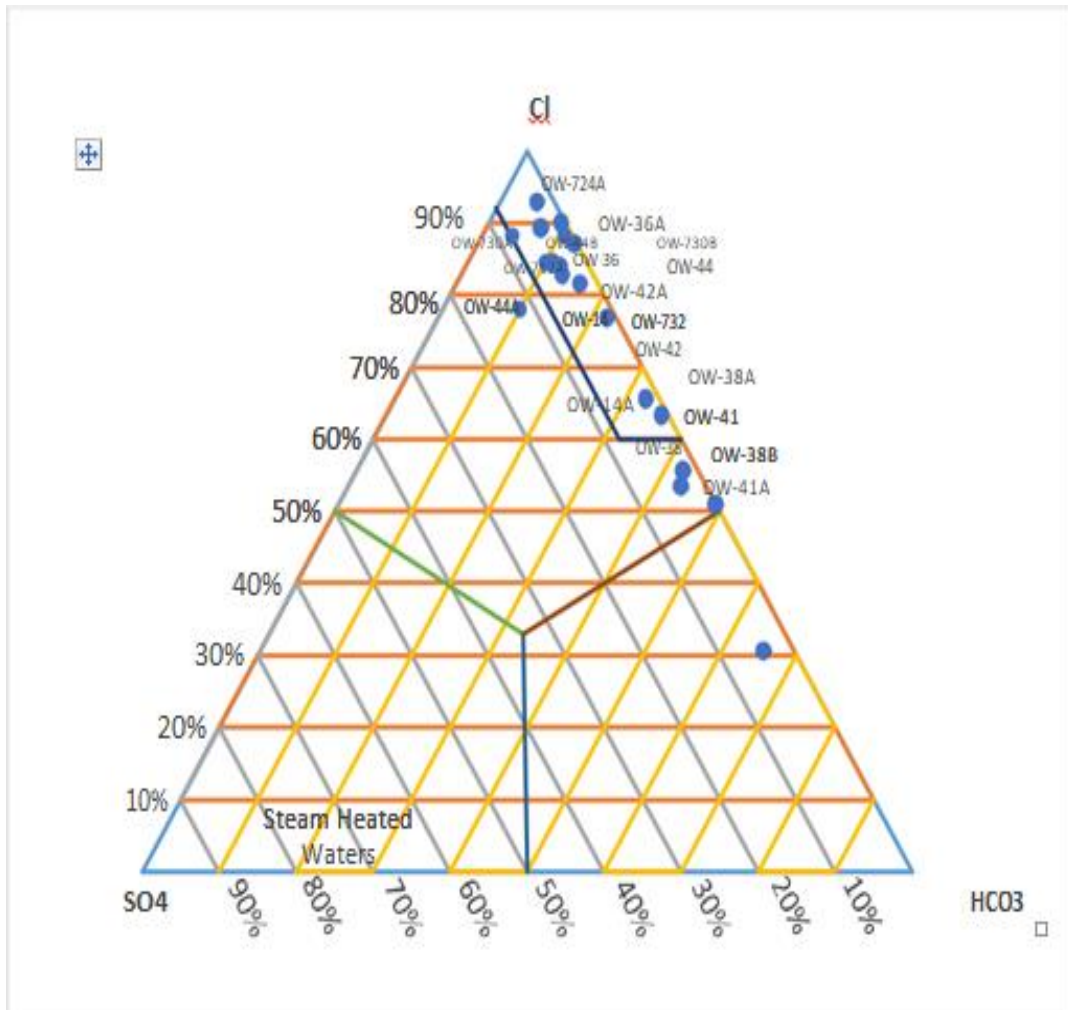


Figure 2.2: Olkaria East fluid classification
(Source: KenGen field reservoir data)

2.4 Hypothetical background on scaling depositions

In light of isotopic data, it is widely agreed that geothermal water is typically transient in nature. As the brilliant water soaks into the earth, it reacts with the hot host rock below, altering the geothermal water's properties. Because of the water-rock relations, the stone minerals disintegrate into the geothermal water, resulting in harmony (Arnorsson S. , 2010). As geothermal water is heated, it rises from the more blazing profound zone to the surface, rich in broken up minerals. The geothermal liquid cools as it moves through rocks and cracks due to conductive heat transfer, and it may begin to bubble near the surface due to a loss of hydrostatic head. When broken down solids become mineral deposits in geothermal fields and hardware, they have an effect on geothermal resource exploitation. Mineral deposition is a major problem in geothermal resource production. Since silica, calcite, and sulfides are common mineral deposits in geothermal systems, such as reservoirs, liners, production casing, and surface gear, it's crucial to understand how they form (Brown, 2011a).

2.5 Conditions and mechanism of formation of silica scales

Direct deposition and colloidal deposition are the two mechanisms by which silica scales form in geothermal applications. The interaction of the silicic acid's siloxane bonds with the metal surface is necessary for direct deposition. This reaction is catalyzed by hydroxyl ions and occurs at high pH levels ($\text{pH} > 8$). Colloidal deposition, on the other hand, occurs through a condensation-polymerization process from silicic acid due to increasing super saturation and creates a stiff, dense, and vitreous layer estimated to contribute 0.5mm/yr of scale (Sinclair L. , 2012). This formation pathway forms small molecular weight dimers and trimmers prior to forming rings of various sizes, and cross-linked polymeric chains and ultimately a complex and amorphous

product. Coagulation and flocculation induce the development of significantly bigger colloid particles after the polymerization steps (Bergna & Roberts, 2010).

Deposition is mainly affected by the silica concentration, temperature and pH; flow rates, aeration and ion effects are also important factors. The operational conditions are kept in the scaling-free zone. Silica is deposited in a number of forms at various depths, including quartz, chalcedony, crystallite, and amorphous silica. Quartz has the lowest solubility and is the most stable form of silica. At the prevailing reservoir temperature, deep geothermal water is generally in equilibrium with quartz. Due to the slow rate of formation, quartz deposition in wellbores and surface equipment is not a common issue. Amorphous silica, on the other hand, is related to temperature fluctuations in geothermal water. Steaming extraction and fluid cooling take place at this stage (Chen & Marshall, 2013).

When precipitated on surface equipment such as pipelines, separators, turbine nozzles, heat exchangers, and re-injection wells, amorphous silica from supersaturated water is the most problematic scale. This problem is more problematic in high-enthalpy geothermal fields, where steam separation occurs and initial silica concentrations are higher. To prevent silica scaling in the pipelines and separator, most fields run the steam separator below the amorphous silica line, under-saturated. Scaling can occur if you work above the amorphous silica line, but at different rates depending on the water composition, retention period, and other factors (Axelsson & Gunnlaugsson, 2010).

Calcium carbonate deposition from geothermal fluid is a major concern in a variety of geothermal fields, largely due to geothermal well plugging. Calcite, aragonite, and vaterite are the most common polymorphs of calcium carbonate minerals. In a

supersaturated calcium carbonate solution, Vaterite is the first mineral to form, but it is brittle and recrystallizes to form the more stable calcite. Calcite and aragonite are the most common calcium carbonate deposition minerals, with the former dominating (Arnorsson & Stefansson, 2013).

In low-enthalpy geothermal fluids, the process that causes sulphide deposition varies from that in high-enthalpy geothermal fluids. Low-enthalpy fields with high dissolved solids concentrations can cause mild corrosion of steel production casings, releasing iron. As a result of scaling, the migrated iron reacts easily with sulphide-rich geothermal fluids, resulting in a higher rate of metal sulphide scale deposition. Sulphide mineral deposition is caused by sulphide-forming metals such as iron and some other base metals in a high-enthalpy geothermal environment (Fe, Zn and Pb). As sulphide forms as a secondary product on nickel and chromium, there's a risk that a problematic scale will develop, causing localized corrosion or sulphide stress corrosion cracking. Since it combines with silica scaling, sulphide depositions in high enthalpy resources can be extreme in water with high Total Dissolved Solid (TDS) content. Metal sulphides and oxides are often deposited directly from geothermal fluids in high-enthalpy systems when the phase or pH changes (Criaud & Fouillac, 2013).

In the same way as sulphur forms a solid deposition around fumaroles, sulphur forms a solid deposition in surface equipment. Sulphur deposits in power plants, especially in condensers and cooling towers, are caused by geothermal fluids rich in H₂S gases. Depending on its concentration, pH, and temperature, sulphur exchanges between sulphate and hydrogen sulphide. In acidic environments, the reaction is rapid, but in alkaline environments, it is very slow. Sulphur (S) is stored in direct contact condensers, where gases come into contact with oxygen; Sulphur can also clog cooling tower water

delivery nozzles (Kristmannsdottir & Sirgurgeirsson, 2010). Through geothermal wells and pipelines, geothermal fluid is injected into the power plants. Boiling will occur in the reservoirs, liners, and wellbore as the temperature and pressure of the fluid changes, resulting in solid precipitation. Gases are liberated from the liquid phase and degassed into the steam phase during the production of calcite, for example. This generates supersaturation, which leads to the formation of calcite within the wellbore, resulting in fluid constriction. This deposition reduces the flow area, resulting in a reduction in well output and, as a result, a fall in wellhead pressure (Ormat, 2011).

2.6 Geothermal scales formation and deposition

The precipitation of solid scales from the geothermal fluid is one of the most important obstacles in the exploitation of geothermal energy. Scales block flow in a number of areas, including boreholes, two-phase pipes, separators, waste water lines, and steam pipelines. Their shape makes it impossible to shut and open valves, resulting in leaks. Scale buildup on turbine blades is normal, resulting in higher turbine chest pressures. Deposition from a single phase fluid i.e. injection pipes, deposition from flashing fluid e.g. wells, separators, two phase-pipelines, and deposition by steam carryover i.e. separators, steam lines, and turbines are the three major areas of scale deposition that can be distinguished (Corsi, 2011).

Scaling and silica deposition can occur at any stage in a geothermal power plant's system. The equilibrium condition inside the fluid is disrupted the minute fluid enters the production well casing. Pressure, temperature, and chemical conditions change as fluid travels towards and through the plant, affecting the solubility of various fluid components, resulting in deposition or scaling of multiple distinct species. Some parts of the power plant are more prone to scale than others, and in a geothermal power plant,

the production wells, brine handling and reinjection system, and steam turbine are the most vulnerable. Although deposition and scaling can occur in other parts of the power plant, they are usually not as serious. Production wells are the initial point where the geothermal fluid's pressure is reduced. The pressure that the fluid is subjected to decreases as it goes up the production well. The solubility of many minerals contained in geothermal fluid is reduced by the reduction in pressure in flowing up the well through two main mechanisms:

- A reduction in dissolved gas content and associated pH changes, and
- As the fluid boils, the liquid fraction decreases, resulting in an increase in mineral concentrations and a consequent temperature drop.

Scaling causes dissolved components to separate from solution and float as minute particles attached to a solid surface, such as a pipe wall. The most frequent ingredient that scales out is silica, which looks like sand. Sulfides and metallic carbonates are two other frequent materials. Mineral scales deposited in geothermal producing wells are more likely to be calcite and other related calcium compounds. Production well scaling can be a serious issue in geothermal power plants since it restricts the flow of geothermal fluid delivered to the power plant, resulting in a decrease in power output. Calcite scaling can occur as the pH of geothermal liquid rises as gases like hydrogen sulfide and carbon dioxide transition from the liquid to the gas phase. Calcite scaling can also develop when the concentration of calcite in the boiling liquid surpasses the saturation threshold due to steam losses in either the reservoir or the production well (Arnorsson, 2013).

It is required anyone to know the following in order to assess the general characteristics of scale formation in a specific water sample:

- The total dissolved solids (TDS),
- pH,
- Temperature,
- Pressure
- Calcium hardness, and
- Alkalinity

Total dissolved solids (TDS) are a typical indicator of a water source's quality. Water quality issues are more likely to emerge as total dissolved solids rises. Other signs will determine if these issues are on the scaling or non-scaling end of the spectrum. Most groundwater have a pH value that ranges from about 5.0 on the acid side to 9.0 on the alkaline side. At pH values greater than 7.5, scaling issues are typical.

Temperature and pH variations can cause scaling to occur. Carbon dioxide dissolved in the geothermal fluid is spontaneously emitted in small amounts when the fluid is flashed to produce steam in separators. Because the pH rises as a result of carbon dioxide emissions, this produces a positive feedback loop, resulting in increased scaling of dissolved fluids (Corsi, 2011).

Mineral deposition scaling is a common problem in almost all production wells. Both reservoir permeability and well productivity are affected by the most serious scale problems. It can be found on any surface that comes into contact with the brine. X-ray diffraction has been used to classify the main minerals deposited within the production lines in many experiments on downhole scale characterization. Calcium, silica, and sulphide compounds are the most common scale species found in geothermal brine (Sinclair L. , 2012). Calcium carbonate and calcium silicate are two calcium compounds that are frequently encountered.

In higher temperature resources, metal silicate and metal sulfide scales are common. Zinc, iron, lead, magnesium, antimony, and Cadmium are common metals found in silicate and sulphide scales. Silica can cause even more problems because it creates an amorphous silica scale that is unrelated to other cations. All of these scales can cause geothermal plants to have difficult operating problems (Arnorsson, 2013).

2.6.1 Factors affecting the formation of amorphous silica scaling

Amorphous silica scaling would potentially be deposited in a water-dominated geothermal system with a high concentration of dissolved silica. The deposition of amorphous silica is highly dependent on temperature and pH of the fluid. The process of silica scaling formation at the surface facilities of geothermal power plants is controlled by temperature, pressure and pH solution change.

Temperature and pressure: The decrease in both temperature and pressure results in decrease in the solubility of amorphous silica in the geothermal fluid leading to deposition of the silica scales on the steam pipes.

pH: The solubility of amorphous silica scales in the geothermal fluids increases with increasing pH in the fluids hence preventing deposition of the amorphous scales in the steam pipes.

2.6.2 Methods of detecting solid deposits

When the well output decreases or wellhead pressure drops, it's time to run down-hole logs to find out what's going on. To detect the location and thickness of solid deposition in a wellbore, different methods have been used. To assess the location and thickness of deposition, caliper logging tools and Go-devil tools are widely used. Caliper logging tools have an electric motor that opens the arms after the tool is lowered into the hole.

The arms center the tool in the well, and variable resistance senses the location of the spring-loaded arms. Because of the temperature limitations of electrical cables and equipment, this procedure necessitates quenching the well with cold water (Molina, 2012).

2.6.3 How scale build-up impacts heat transfer

Making sure the plant machinery used in geothermal operations is working properly is one way to save money on electricity. As mineralized water is passed through steam pipes at a high temperature, the impurities in the water precipitate out onto the inside, causing scale to form. Impurities are accumulated even more readily on the interior of the steam pipes as the water begins to boil. Scales are formed when deposited impurities accumulate over time. The pumping power needed to transfer water through the steam pipes increases as the diameter of the pipes narrows due to scaling. Scaling also raises the pipe's thermal resistance, which means it requires more heat to boil water or more cooling to cool it down. Scaling has the effect of rising energy prices due to lower efficiencies. Scaling removal from the inside of pipes is a time-consuming, labor-intensive, and costly process. It is less costly to treat water to avoid scale buildup rather than to try to extract scale after it has formed. When scale builds up inside pipes, it takes more energy to heat or cool water, and when scale is allowed to build up inside pipes, the resistance to heat transfer increases cumulatively.

This means that as the device becomes less efficient, the amount of energy needed to heat or cool water in the scaled pipes increases. When water has not been treated to minimize hardness, scale accumulates over time and is frequently followed by corrosion and further narrowing. When pipes go unchecked, water process temperatures

can become more difficult to regulate, and inefficient heat transfer processes waste energy and cost more (Mahon, 2010).

2.6.4 Silica scale deposition

Silica (SiO_2) and calcite (CaCO_3) are two of the most popular geothermal scales. These two scales are both white and difficult to distinguish visually. Small amounts of iron sulphide, a scale deposition product found inside all geothermal pipelines, give the silica scales a grey or black appearance. If bubbles form when a drop of hydrochloric acid is dropped on a piece, it is calcite.

After super-saturation, silica scale deposition from geothermal fluids can take minutes or hours, according to (Mecardo & Hurtado, 2011). This is why silica deposition has been discovered in many geothermal facilities' fluid handling equipment. As a result, unlike calcite, which tends to precipitate shortly after reaching super-saturation during flashing, silica deposition can be kinetically regulated and delayed by minutes or hours after saturation is reached.

Silica scales can be found in all geothermal installations to some extent, however the scaling rate is relatively low when the temperature is kept above the solubility threshold for amorphous silica (the non-crystalline form of silica), which is one of the design criteria for most geothermal plants. The concentration of silica in the reservoir is usually in balance with quartz, the crystalline form of silica. The concentration of silica in the water increases as the water boils and cools. The water becomes quartz supersaturated almost immediately, but no quartz precipitates form due to the slow formation of quartz crystals. Amorphous silica deposition is the most common and problematic scale that forms when geothermal water is heated to high temperatures. Many scholars have looked into this scale (Were & Tsao, 2010). (Hurtado, et al., 2010). The analysis of

silica scale formation has received a lot of attention because the efficient extraction of energy from high-temperature geothermal resources is restricted by the silica scale that can form as a result of cooling (Fournier & Rowe, 2012) (Mahon, 2010) discovered that aqueous silica concentrations in high-temperature geothermal fluids are controlled by a close approach to equilibrium with quartz. Extensive experimental tests on the quartz solubility constant have been performed (Fournier R. O., 2013) (Fournier R. O., 2012). The solubility of quartz increases as the temperature rises. Quartz is often not found as a primary mineral in geothermal systems, but rather occurs as a result of water precipitation. Silica scales are only known to form if the aquifer water has been sufficiently boiled and cooled to saturate it with amorphous silica, due to the quick rate of deposition of this phase compared to quartz, particularly below 150°C. Amorphous silica deposition, unlike calcite scale formation, does not occur at depth in production wells, but rather in wellheads, surface piping, and injection wells.

Since quartz solubility regulates silica concentrations in high-temperature geothermal waters, aqueous silica concentrations in producing aquifers rise as the water temperature increases. As a result, the temperature at which amorphous silica saturation is reached in specific well water is determined by the temperature of the source aquifer. The degree of super saturation, temperature, and salinity all influence the rate of amorphous silica precipitation and colloidal formation polymerization. Aeration may also help. In amorphous silica oversaturated solutions, silica molecules can react with one another to form colloidal silica or deposit from the solution to form. Many experiments have been performed on the solubility of pure amorphous silica (Fournier & Marshall, 2011).

The solubility of amorphous silica is determined by the ions that influence its surface charge. The effects of dissolved salts of varying concentrations on the solubility of amorphous silica have been studied by (Marshall & Warakowski, 2014) and (Chen & Marshall, 2013). They discovered that the influence of the salt cations on amorphous silica solubility decreased in the following order: $Mg^{2+} > Ca^{2+} > Sr^{2+} > Li^+ > Na^+ > K^+$ (Yakoyama, Takahashi, Yamanaka, & Tarutani, 2011), demonstrated that the aluminium ion can have a substantial effect on the rate of silica polymerization. The formation of complexes between silica and cations in the salts is likely to be the cause of these effects, but the salts will also influence the value of the activity coefficients taken by aqueous silica species. The structure of and precipitated amorphous silica, as well as its solubility, can be influenced by the presence of cations in solution.

Polymeric silica is less likely than monomeric silica to precipitate out of solution. The effectiveness of polymerization treatment in reducing amorphous silica deposition from spent geothermal waters is determined by the relative rates of the two reactions, amorphous silica deposition and silica polymerization, as well as the rate at which polymeric silica settles from solution. In the Olkaria I, II, and III geothermal wells, silica scales have been found. It's contained in wellhead equipment, separated water, and the plant in all cases. Maintenance issues with silica scale formation in heat exchangers, brine pipes, and first stage turbine nozzles were recorded in (Opondo & Ofwona, 2013). In Olkaria, (Opondo & Ofwona, 2013) reported extensive silica deposition in one well's wellhead equipment.

2.6.5 Amorphous silica

Amorphous silica is one of the most common scaling problems in geothermal power plants since its solubility decreases with decreasing temperatures. Amorphous silica

scales can form anywhere from production wells to surface facilities to injection wells downstream, depending on the conditions (Erlindo, 2011). It is common practice to maintain the temperature of geothermal installations above the saturation point for amorphous silica to avoid amorphous silica deposition. The amount of heat that can be extracted from the fluid discharged from production wells is limited as a result of this (Erlindo, 2011).

The concentration of silica in the brine rises as it passes through flash vessels, and the temperature of the brine drops even more. Silica is oversaturated under these conditions and will either precipitate as amorphous silica or react with available cations (e.g. Fe, Mg, Ca, Zn, etc.) to form co-precipitated silicate deposits. The flow of fluid from production wells, flash vessels, binary units, and the injection system is severely hampered by these deposits. In addition to reducing flow, silica scaling has a major effect on heat transfer in binary unit equipment (Burton, Bourcier, Burton, & Leif, 2013).

If geothermal waters become oversaturated in amorphous silica, two types of processes are likely to occur: - The first is monomeric silica deposition directly onto a surface, and the second is monomeric silica polymerization to form silica polymers. The process that occurs in spent high-temperature geothermal waters is affected by the water's environment to some degree (Gunnarson, Ivarsson, Sigfusson, Thrastarson, & Gislason, 2010). Silica scaling is likely to occur in turbulent flow where there is surface available for monomeric deposition onto the surface, but if the waters are put in a quiet environment, silica polymerization is the preferred method.

Brine in the reservoir is in equilibrium with quartz, but as the fluid moves up the well, it becomes supersaturated with amorphous silica due to boiling, and monomeric silica

starts to polymerize after a time known as the "induction period." Aside from preventing over saturation, research on the silica induction cycle and polymerization rate have aided in the development of other approaches to managing silica precipitation from geothermal brines (Erlindo, 2011). These include:

i. acidification to lower the pH, ii. Brine aging to transform monomeric silica to colloidal silica, iii. The use of inhibitors that claim to avoid or minimize silica scaling, iv. Silica precipitation with lime or by bubbling CO₂ through the solution, v. Mixing the brine with steam condensate, vi. Coagulation to eliminate colloidal silica, and vii. Maintaining the temperature of the brine above the silica super saturation temperature by changing and regulating separator pressure.

2.7 Types of Scale

2.7.1 Calcium carbonate scales

Calcium carbonate scales, i.e. crystalline calcium carbonate scales Calcite is commonly discovered in wells with reservoirs of 140-240°C, and is primarily found when the water in the well begins to boil. This scaling is caused by CO₂ degassing and an increase in pH as a result. Calcite has retrograde solubility, meaning it is more soluble at lower temperatures than it is at higher temperatures, therefore when the water and steam go up the well, the calcite abruptly stops and forms scales. Calcite scales are found largely in a 200-300m long area of the well above where flashing, or rapid conversion of water to steam, occurs, but not below or above that region. This makes calcite scale control easier, and chemical modeling can be used to anticipate them rather precisely. Because calcite scaling requires a certain level of super saturation, there is a tiny window of opportunity in this scenario, as almost all geothermal water is at equilibrium, or saturated with regard to calcite in the reservoir. Calcite scaling is usually not a problem

in wells that produce from reservoirs with temperatures greater than 260°C because the amount of dissolved calcite in the water is lower at higher reservoir temperatures. More complicated minerals, primarily metal sulfides, silicates, and oxides, can form scales at temperatures above 300°C, especially in extremely saline water (Solis, 2010).

Many geothermal fields are considered to have problematic calcium carbonate scale formation (Simmons & Christenson, 2012). Scale formation of this kind is expected to be most extreme at the depth level of first boiling, according to (Arnorsson, 2013). This form of deposition can greatly reduce the production of wells or even clog them. Calcite deposition has been found in two phase lines where fluids from two separate wells combine in other unusual occurrences. Calcite deposition can also occur as a result of the re-injected fluid being heated.

Although the water in the aquifer of high-temperature geothermal systems is similar to becoming calcite saturated (Arnorsson, 2013) (Karingithi & Opondo, 2011), equilibrium between calcite and solution is easily reached at these temperatures. Calcite saturated waters will become oversaturated after substantial boiling of the aquifer water and subsequent CO₂ degassing. The effect of degassing during adiabatic boiling is counteracted by increasing calcite solubility with decreasing temperature. Calcite scaling problems have been successfully solved around the world, either by mechanical cleaning or the use of inhibitors (Pieri, Sabatelli, & Tarquini, 2011).

2.7.2 Iron silicate scales

If the fluid contains a large amount of iron, deposition of iron silicates will begin at a higher temperature than silica deposition, but at lower temperatures, iron will be deposited as oxides. In saline geothermal fluids or fluids disturbed by volcanic gas, they commonly form with sulphide scales. These scales do not usually form at pressures

higher than 16-18 bars, and are kept at bay by keeping the wellhead pressure above that level (Thorhallsson, 2012).

2.7.3 Sulphide scales

Sulphide deposits are likely to form in saline geothermal fluids or fluids disturbed by volcanic gas effects due to metal(s) reactions with H₂S. PbS (galena), ZnS (wurtzite, sphalerite), CuS (covellite), Cu₂S (chalcocite), CuFeS₂ (chalcopyrite), and bornite (Cu₅FeS₄) are the most abundant in saline solutions. The most popular sulphides where volcanic gas affects the system are FeS₂ (pyrite) and FeS (pyrrhotite). In several geothermal fields, galena, chalcopyrite, pyrrhotite, and traces of bornite have also been found (Armannsson & Hardardóttir, 2010). There have been no concrete steps taken to deal with such deposits.

2.8 Methods for controlling scales deposition

Several methods have been developed and adapted to minimize or remove amorphous silica deposition in geothermal installations. Maintaining steam separation pressures and temperatures above silica saturation is a typical method for reducing amorphous silica scaling in production wells and wellhead equipment. Many other methods have been used, including:

- **pH modification;** Controlling silica deposition by pH modification has long been recognized as a useful, although costly technique. Depending on whether the pH is raised or lowered, there are two methods. Increasing the pH of silica saturated brine to > 8.5 through the addition of alkali significantly increases the solubility of amorphous silica, making the brine silica under-saturated, while decreasing the pH through the addition of acid delays the rate of polymerization of silica in the saturated brine, and thus also delays the rate of silica deposition

from the brine. Increasing the pH achieves full control over deposition by adjusting the solubility of amorphous silica, while adding acid merely extends the time before supersaturated silica deposits. Despite this, because of the cost benefit, acid treatment with mineral acids is still favored over alkali dosing (Brown, 2011).

- **Chemical inhibition;** some types of scale deposits can be significantly reduced or removed by injecting a chemical scale inhibitor down hole. In contrast to mechanical controlling methods for calcite, scale inhibition is a promising system both technically and economically. In the application, choosing an effective inhibitor and a method for injecting it into the well is important (Pieri, Sabatelli, & Tarquini, 2013). Any deposition is reduced, delayed, or prevented by the inhibitors. This approach involves running a coiled tube into the well below the scaling plug and continually dosing the chemical into the well. The inhibitors react against solid deposition in one of these two ways: they prevent deposited crystals from adhering to a surface and they absorb onto the surface of incipient crystals, distorting the crystal structure and preventing it from developing.
- **Precipitation of silica prior to re-injection;** There are many methods for precipitating silica from waste brines prior to re-injection, all of which clearly provide a high degree of protection against silica deposition in downstream piping and re-injection facilities. Although these options are usually capital intensive, the potential commercial value of silica and other chemical products that can be recovered can offset plant operating costs.

- **Flash crystallizer clarifier;** Flash crystallization is a kinetic method of managing solids deposition that was developed by UNOCAL and Bechtel in the early 1980s for handling highly saline geothermal brines (20-30 percent total dissolved solids, TDS) at the Salton Sea. This approach is based on the principle that if solids deposition can't be stopped, it should be allowed to happen on solid particles carried by the brine rather than settling out on plant surfaces (Brown, 2011) (Barnett & Garcia, 2010).
- **Turbine washing and steam scrubbing;**
As any water carry-over from the separators dries out as the steam expands in the inlet nozzles, turbines are prone to scaling. Scaling decreases the amount of steam mass flowing through the turbine by narrowing the throats of turbine nozzles. This has a direct effect on turbine output or electric power generation. While the machine is working, the deposition can be extracted by turbine washing. A mist is produced by injecting clean water from the condensate into the incoming steam line, eroding any solid deposition from the turbine nozzles and blades. Water injection accounts for around 5% of the total mass of steam entering the turbine. It is important to provide clean water that is oxygen-free and has a low level of total dissolved solids (TDS), as contaminated water can create more problems than it solves. Steam scrubbing, which involves injecting clean water into the incoming steam line before the final separator, is often used to improve steam purity. This works well in reservoirs with a lot of steam or for dry steam.
- **Silica suppression;** by lowering the pH of the solution and diluting it, through condensate mixing will minimize silica scaling (Hirowatari & Yamauchi,

2012). The molecular deposition rate is reduced to 0.01mm/yr by mixing 50 tons/hr of water with 17.5 tons/hr of 60-degree condensate. All super-saturation in 175-degree water is eliminated by mixing with an equivalent volume of 60-degree condensate. Dilution can influence silica scaling, according to the results of this experiment. Simply inject condensate into the brine disposal line to reduce silica concentration below amorphous silica saturation. This is neither costly nor time-consuming to plan.



Figure 2.3: Turbine blades with silica deposits on nozzles from Olkaria II power plant
(Sources: KenGen, 2014)



Figure 2.4: Steam valve with silica scales from Olkaria II power plant
(Source: KenGen, 2014)

2.8.1 X-ray diffraction (XRD) characterization of solid scales deposits

The atoms are arranged in a regular pattern, and there is a smallest volume element that describes the crystal by repetition in three dimensions. A unit cell is the smallest volume element in the system. The unit cell's dimensions are described by three axes. A pure substance's X-ray diffraction pattern is thus like a fingerprint of the substance. Polycrystalline phases are characterized and identified using the powder diffraction method. As standards, diffraction patterns have been gathered and saved on magnetic or optical media. The main use of powder diffraction is to identify components in a sample by a search or match procedure, the areas under the peak are related to the amount of each phase present in the sample (Meier, 2011). When an X-ray beam hits an atom, the electrons around the atom start to oscillate with the same frequency as the incoming beam. In almost all directions there will be destructive interference, that is, the combining waves are out of phase and there is no resultant energy leaving the solid sample. However the atoms in a crystal are arranged in a regular pattern, and in a very few directions we will have constructive interference. The waves will be in phase and

there will be well defined X-ray beams leaving the sample at various directions. Hence, a diffracted beam may be described as a beam composed of a large number of scattered rays mutually reinforcing one another (Meier, 2011)

CHAPTER THREE

MATERIALS AND METHODS

3.1 Overview

This chapter includes the research layout, equipment's used in the experiment and the standard methods used for sampling two-phase geothermal fluids for chemical analysis and scale deposits identification and structural characterization process. The geothermal fluid samples were collected from three selected points at the power plant .i.e. before separation of the steam from the brine at the separator, after steam separation (dry steam at the turbine inlet) and at the turbine exhaust (steam condensate). The samples were collected from these points for three days each giving six days set of results as tabulated in Appendix 1. An average of the six days tabulated results at each collection point was calculated and presented in Tables (4.1 – 4.10) as representation of all three selected areas in the power plant.

3.2 Sampling equipment

Brine and steam samples were collected using Webre separator because of its convenience for sampling two-phase wells. This was done by adjusting the brine levels in the separator which makes it possible to collect each phase separately .i.e. low brine level for gas and high level for brine. Plastic sample bottles were used for sampling because they were convenient for sampling geothermal fluids since they are unreactive with the samples inside, they were used throughout to store geothermal samples. Amber glass sample bottles were used for collecting strainer, CO₂, pH and conductivity analysis samples while cooling coil was used for collecting steam condensate samples and finally gas flasks were prepared by adding 50ml 40% NaOH prior evacuation using a vacuum pump.

3.3 Sample treatment and preservation

Treatment and preservation of hydrothermal samples was subdivided into two major procedures: physical and chemical. In the physical procedure, filtration involved removal of solid particles using in-line filters which were critical for samples that would be acidified and also for the ones that would undergo ion chromatography analyses. Freezing was undertaken to stop biological activities while cooling was necessary for carbonate and pH samples analyses. Airtight containers were used to prevent loss of volatile constituents such as CO₂ and H₂S and immediate analysis was critical for redox sensitive species such as H₂S, pH and volatile components. On the other hand, chemical procedure entailed acidification to prevent adsorption of cations to negative charges on the walls of plastic containers while precipitation prevented interference between species, and this was achieved by adding zinc acetate to sulfate analysis samples to avoid oxidation of H₂S to sulfate ions and finally, gas fixation involved gas flasks pre-filled with an aliquot of 40% NaOH to trap CO₂ and H₂S and this was to increase the volume of steam collected in the evacuated port of the flask.

3.4 Sampling procedure

Sampling of geothermal fluids was carried out in three different locations as follows: The brine samples were collected from the wellhead before steam extraction at the separator, dry steam samples from the turbine inlet after being recovered from the brine, and steam condensate samples from the turbine exhaust. The approach involved connecting a Webre separator 1.5 meters from the wellhead to a two-phase steam pipe that carried complete discharge to an atmospheric silencer and recording sampling pressure and temperature. The flow diagram is given in Figure.3.1.

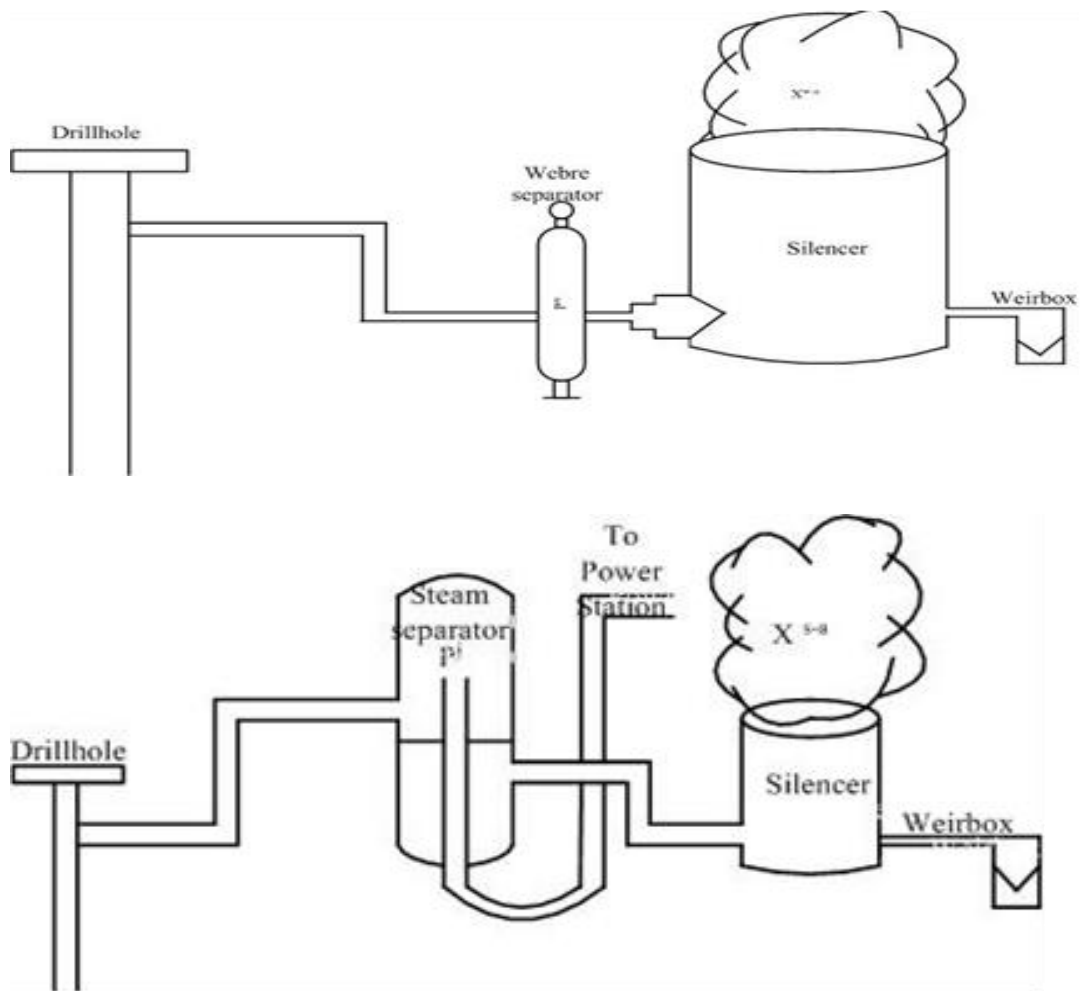


Figure 3. 1: Schematic diagrams of a two-phase pipeline that carries well discharges from the wellhead to an atmospheric silencer
(Source: KenGen, 2014)

During sampling, a chromium steel Webre separator was connected to selected points along the steam line of the wellhead plants using a horizontal discharge testing technique to obtain steam and water samples. The experimental set up of the Webre separator is depicted in figure.3.2 (a) and (b).



(a) Webre separator connected to a two-phase steam pipe



(b) Collecting brine and steam samples

Figure 3.2: Experimental set up of a Webre separator

Some steam was pumped through the sampling apparatus prior to sampling the geothermal fluid to clean and remove any contaminants.

3.5 Chemical analysis of the brine and steam samples

Standard techniques used to analyze the samples in the laboratory included titrimetric, spectroscopy, chromatography, and the molybdosilicate process, which was used to analyze silica (SiO_2). Samples for all components, except pH, CO_2 , and H_2S , were filtered on site using $0.45\ \mu\text{m}$ filter papers into low density polyethylene bottles using a polypropylene filter holder to avoid contact with any suspended matter. Gas samples were collected in pre-weighed 325-340 ml evacuated gas sampling flasks containing 50 ml of 25% w/v NaOH solution to react with the main condensable gases (CO_2 and H_2S), while non-condensable gases (CH_4 , H_2 , N_2 , and O_2) occupied the head space. Water samples were treated at the time of collection, depending on the parameters that needed to be analyzed. pH, Total Dissolved Solids (TDS), conductivity, Total Carbonates' Carbon (TCC), Chloride, and Fluoride samples were obtained and stored without treatment. To prevent polymerization of monomeric silica, samples for Silicon IV Oxide (SiO_2) analysis were diluted ten times in deionized water. Significant aqueous cations (Na^+ , K^+ , Ca^{2+} , Mg^{2+} , Al^{3+} , Li^+) and anion (SO_4^{2-}) were analyzed using ICP-AES and ICP-MS after samples were filtered through a $0.45\ \mu\text{m}$ Millipore membrane. Cation samples were stored in 1ml nitric acid, and for SO_4^{2-} analysis, 2ml of 0.2 M Zn-acetate solution was added to the samples to precipitate the sulphides in the form of ZnS. The following analyses were carried out on the samples:

3.5.1 Determination of pH

The pH of brine samples was determined by first calibrating the pH meter using standard buffer solutions. After calibration, the glass electrode was rinsed with distilled water before dipping into the sample bottle and the 'measure' button was clicked. The

pH value of the water sample was recorded after the pH meter had stabilized. The glass electrode was rinsed with distilled water before proceeding to subsequent samples.

3.5.2 Determination of H₂S

Since H₂S is a volatile component, its analysis was carried out in the field immediately the moment it was sampled. H₂S was first determined by pipetting a suitable aliquot of the brine sample into a clean conical flask followed by adding 5 ml NaOH and 5 ml acetone to the sample, then a small amount of the indicator was added till the solution turned tinge yellow. Finally, the sample was titrated against 0.001M mercuric acetate to a pink end point, the titre volume was recorded and the H₂S concentration was determined.

3.5.3 Determination of CO₂

The CO₂ in the geothermal fluid samples was determined first by measuring a suitable volume of the sample into a beaker with stirring bar and initial pH measured. Sufficient 0.1N AgNO₃ was added to remove all H₂S and pH was adjusted to 8.3 using 0.1N HCl if initial pH was above 8.3 and NaOH if initial pH was lower than 8.3 and finally titrated with standard 0.1N HCl down to pH 3.8 and recorded titre (T).

3.5.4 Determination of conductivity and total dissolved solids (TDS)

Both parameters were measured using a conductivity meter and are used to assess steam quality. TDS is best determined gravimetrically since conductivity meters only account for charged species (Na⁺, Ca²⁺, Cl⁻, HCO₃⁻) but disregards neutral species, most importantly H₄SiO₄.

3.5.5 Determination of high chloride > 20 ppm

Chloride concentration within a high range was determined by Mohr titration, this is the traditional method for analyzing chloride and is simple, accurate technique. The chloride in the geothermal fluid samples was first determined by pipetting 10 ml of the sample into 100 ml beaker, added 1 drop of 0.5 ml zinc acetate to remove H₂S and 2 – 3 drops of chromate indicator. Finally, the sample was titrated against 0.1 M AgNO₃ until a permanent change in color was observed, from yellow to red-brown and the titre volume was recorded.

3.5.6 Determination of high silica >20 ppm

The silica in the samples was first determined by pipetting 5 ml of the samples into 50 ml plastic volumetric flasks, reagents and distilled water were used to make the blank. 2 ml 6N HCl and 5 ml ammonium molybdate solution was added to the samples and left for about 15 minutes for the reaction to occur, then distilled water was used to fill the gap and finally the concentration of silica was determined by measuring the absorbance at 410 nm (SiO₂ was equal to concentration dilution factor).

3.5.7 Determination of low silica < 20 ppm

The low silica in the samples was determined by first pipetting 10 ml of the sample into 50 ml plastic volumetric flasks and a blank was prepared using distilled water and reagents, then 10ml molybdate-acid reagent was added to the samples and reagent blank. The solution was allowed to stand for about 10 minutes for reaction to occur before 2 ml of A.N.S.A solution was added and solution mixed thoroughly, then after about 5 minutes, absorbance was measured at 410 nm to obtain silica concentration.

3.5.8 Determination of sulfates (SO₄²⁻)

The ion sulfate was determined using a turbidimetric process. In an acetic acid medium, sulfate was reacted with barium chloride (BaCl₂) to form a barium sulfate suspension:



The spectrophotometry was used to determine the absorbance of the suspended solids, which was proportional to the sulphate concentration. The detection limit was estimated to be around 1ppm. The sulfate in the samples was first determined by pipetting 5 ml of the sample into 50 ml volumetric flasks and prepared a blank using distilled water and reagents. 3 ml of buffer solution was later added to the samples and blank, then 0.2-0.3 g of barium chloride was added while stirring and distilled water was used to top up to the mark. Within 5 minutes after the addition of barium chloride, absorbance was measured at 425 nm to obtain sulfate concentration.

3.5.9 Determination of Boron

The boron in the geothermal sample was determined by first pipetting 0.1 ml of the samples into plastic beakers, then distilled water and reagents were used to prepare a blank. 3 ml of curcumin and acid solutions were later added to the samples and blank, then the solution was left for about 1 hour, swirling being done at intervals of 20 minutes. Later, 15 ml of buffer solution was added and left to cool before taking absorbance measurement at 540 nm to obtain boron concentration.

3.5.10 Determination of low chloride < 20 ppm

Low chloride concentration was determined by the ferric thiocyanate method. This is a colorimetric method. Chloride reacts with mercuric thiocyanate, liberating thiocyanate ion which in the presence of ferric ion (ferric ammonium sulphate) produces a red

colored ferricyanogen complex. The chloride in the samples was determined first by pipetting 20 ml of the sample into 50 ml glass volumetric flasks, then used distilled water and reagents to prepare a blank. 2 ml of 0.25M Fe (NH₄) (SO₄)₂.12H₂O and Hg (SCN)₂ solutions were added to the samples and mixed thoroughly, then the solution was left to stand for about 10 minutes to allow for the development of color and finally absorbance measurement was taken at 480 nm to obtain chloride concentration.

3.5.11 Determination of fluoride ions

The fluoride ions in the samples was determined by first transferring 10 ml of the sample into 50 ml beaker, then 10 ml of TISAB 1:1 was added and fluoride electrode was immersed in the sample while stirring continuously. The reading was allowed to stabilize before reading the sample concentration from the meter.

CO₂, total carbonate carbon (TCC), and H₂S were determined in water samples using a titration technique with 0.05M HCl and 0.001M Hg-acetate, while chloride was measured using the argentometric Mohr's method with AgNO₃. The hydrogen sulphide (H₂S) was calculated using a dithizone indicator and a titration with Hg (CH₃COO)₂ solution. When the color changes from yellow dithizone in an alkaline solution to pink Hg-dithizonate, the end point has been reached (Arnorsson & Stefansson, 2013).

Potentiometric titration was used to calculate the CO₂ concentration. A small amount of the solution from the Giggenbach bottle containing the NaOH solution and condensed steam was accurately measured and diluted with deionized water to around 50 ml. The pH was regulated to around pH 9 with 1M HCl solutions, and then titrated to pH 3 with 0.1 M hydrochloric acid using an automated titration unit. The titration's equivalence points were pH 8.20 and 3.80, and the amount of acid added between these points was used to calculate the CO₂ concentration in the sample. The Atomic

Absorption Spectrometer (AAS) was used to examine the aqueous cations (Na^+ , K^+ , Ca^{2+} , Mg^{2+} , Al^{3+} , and Li^+). Boron, SiO_2 , and SO_4 were analyzed using a spectrophotometric technique and Ultra-Violet/Visual light analysis. Gas chromatography was used to examine non-condensable gases in the headspace of the gas sampling bulb (Arnorsson & Stefansson, 2012).

Table 3.1: Standard methods used for the analysis of different elements in the collected samples (Arnorsson & Stefansson, 2012)

Analysis	Method
pH	pH meter
Conductivity / TDS	Conductivity meter / gravimetry
CO_2	Potentiometric titration
H_2S	Titrimetric
B	Spectrometry
SiO_2	Spectrophotometry (with ammonium- molybdate)
Na	Atomic Absorption spectrometer (AAS)
K	Atomic Absorption spectrometer (AAS)
Mg	Atomic Absorption spectrometer (AAS)
Ca	Atomic Absorption spectrometer (AAS)
F	Spectrophotometry technique using Ultra-violet/ visual light analysis
Cl	Spectrophotometry technique using Ultra-violet/ visual light analysis
SO_4^{2-}	Turbidometry with barium chloride

3.6 Sampling, analysis, and structural characterization of the scale deposit

During routine maintenance operations, scales deposit were obtained from the separator u-seal, the silencer, and the turbine rotor of the plant. Before analysis, all samples were oven-dried for 24 hours at 105°C and cooled with a desiccant humidifier. The scale samples were identified and characterized using instrumental analytical techniques. Qualitative and quantitative chemical analyses were carried out using the following methods: X-Ray diffraction (XRD analysis) was used to quantitatively analyze the compounds present in the scales deposit samples while X-ray florescence (XRF

analysis) was used to analyze the elemental composition of deposited materials of the scale samples with findings shown in Tables 4.5, 4.7 and 4.9. Following a thorough analysis of geothermal fluid composition and characterization of scale deposits on the plant's Separator u-seal, silencer, and Turbine rotor, an inferential approach was used to determine what was causing scaling deposition on the facilities. Mineral saturation calculations were used to predict scaling potential. As a result, it was important to understand the concentrations of the chemical species involved in scaling, namely SiO_2 , H_2S , Ca^{2+} , and CO_2 . The quantities, operational behavior, and characteristics of each element and compound found in the sampled fluid and scale deposits were the focus of this approach. The data collected, as well as knowledge from the literature, was used to determine what causes scaling and how it affects geothermal energy generation operations. This would then serve as a starting point for developing appropriate recommendations to address the current scaling situation.

CHAPTER FOUR

RESULTS AND DISCUSSION

4.1 Introduction

This section focuses on the presentation of results and discussions from the experimental research carried out in well 37B, Olkaria East field production. Scaling potential in this well was predicted based on mineral saturation calculations using the WATCH speciation program, which is a free software for predicting scaling potential and has a database of all common minerals. The data was analyzed and interpreted using this program and a graph of both amorphous and quartz silica solubility was obtained from which the minimum separation pressure was determined. It was therefore important to determine the concentrations of the chemical species involved in the scaling formation in steam pipes and the chemical composition of geothermal brine because the type of scaling formed in steam pipes depends on these two analyses as shown in the table 4.1.

Scale deposits were also collected from the separator u-seal, silencer, and turbine rotor for identification, structural characterization, and an inferential approach was used to determine what was causing scale deposition in the steam pipes using instrumental analytical techniques. The two-phase brine-steam samples were analyzed in the laboratory using standard methods such as titrimetric analysis, spectroscopy, and chromatography. The scales were subjected to an X-ray diffraction (XRD) analysis in Olkaria geochemistry laboratory, which revealed 23 angstrom on the 2D- θ scale, which is the characteristic for amorphous silica.

4.2 Physical and chemical composition of brine samples before steam extraction at the separator

Table 4. 1: Brine sample analysis data before steam extraction at the separator

Elements are identified as ions

Brine sample analysis before steam extraction at the separator							
Mean values							
Sampling point	Discharge enthalpy	Total dissolved solids (TDS) ppm	pH@22°C	Silica (SiO ₂) ppm	Sulphate (SO ₄ ²⁻) ppm	Iron (Fe ²⁺) ppm	Sodium (Na ⁺) ppm
Wellhead	2449	1140	8.33	769	381	41	453
	2407	1080	8.33	708	352	42	426
	2663	1200	8.7	882	389	61	510

As shown in table 4.1, the geothermal brine being discharged from the production wells at high pressure and temperature has a high mineral content from the underground reservoir. As the fluid flows up the wellhead and associated pipelines, boiling takes place because of pressure drop, the temperature of the brine also decreases as it flows through the well to the surface, causing silica solubility to decrease and the brine phase to become oversaturated. As the pressure in the flash vessel decreases, steam flashes, lowering the temperature of the brine even further. The brine phase becomes more concentrated in the flash vessel. Under these conditions, Silica can either precipitate as amorphous silica or react with available cations such as Fe, Mg, Ca, and Zn to form co-precipitated silica deposits. Since its solubility decreases with decreasing temperature, amorphous silica deposition does not occur at depth in production wells, but rather in wellheads, surface piping, and injection wells. This explains why the brine samples collected before steam extraction at the separator contained a high concentration of mineral ion elements and dissolved solids (TDS).

4.3 Physical and chemical composition of steam samples at the turbine inlet

Table 4.2: Steam sample analysis data at the turbine inlet

Elements are identified as ions

Steam sample analysis at the turbine inlet									
Mean values									
Sampli ng point	TDS (pp m)	<u>pH@22</u> °C	Sulpha te ions (ppm)	Chlorid e ions (ppm)	Silicate ions (ppm)	Iron (ppm)	Sod ium ions (pp m)	Potassi um ions (ppm)	Metha ne (ppm)
Turbin e inlet	34.2	5.78	6.2	0.18	48.8	14.1	0.7 2	0.33	1.49
	33.7	6.1	5.9	0.18	49.6	14.7	0.9 1	0.45	1.42
	12.4	5.98	6.8	0.24	50.7	14.9	0.8 4	0.51	0.75

As indicated in table 4.2, the total dissolved solids (TDS) and mineral ions i.e. impurities in the steam present in the turbine inlet are a result of steam carry-over which causes scale deposition on the turbines and other related components exposed to the steam. This is because of the brine droplets that contain the solutes and mineral impurities carried along and then get evaporated on the substratum. This is due to the fact that steam separation from the brine at the separator does not always occur as anticipated. It is because of the anticipated carry-overs in the steam that total dissolved solids (TDS) in the strainer samples must be monitored daily. These samples are collected just before steam enters the turbine. Most solutes are soluble in the liquid phase (brine) which is normally removed at various separator stations making the steam entering the turbine 99 percent pure, therefore TDS in the strainer samples is usually low. High TDS in the strainer samples would conclude brine carry-over. These solutes deposit on the turbine tend to reduce the number of revolutions per second i.e. reduces the efficiency of the rotation of the turbine blades and consequently, low power output.

Table 4.3: Chemical composition of the steam phase

Item	Description	Unit	Mean Value
Impurities in steam	Na	Ppm	0.82
	K	Ppm	0.43
	Cl	Ppm	0.2
	Fe	Ppm	14.6
	SiO ₂	Ppm	49.7
Non-condensable gases (NCGs)	NCGs in steam	Ppm	1.22
Composition of gases in NCGs	CO ₂	ppm	379.2
	H ₂ S	ppm	11.6
	H ₂	ppm	16.15
	N ₂	ppm	70.97
	CH ₄	ppm	1.22

4.4 Chemical composition of steam condensate at the turbine exhaust

Table 4. 4: Steam condensate sample analysis at the turbine exhaust
Elements are identified as ions

Chemical analysis of steam condensate sample at the turbine exhaust			
Mean values			
Sampling point	Total dissolved solids (TDS) ppm	pH@ 22 °C	Conductivity (µs)
Turbine exhaust	3.78	4.34	7.53
	3.76	4.29	7.12
	3.79	4.32	6.19

As demonstrated in table 4.4, all the dissolved solutes and mineral ions carried over in the steam have already deposited on the turbine blades and rotor as the steam rotates the turbine to generate electricity, the steam condensate exiting the exhaust contains

small amounts of TDS and no mineral ion impurities, sulfates, chlorides, or silicon dioxides.

4.5 Structural characterization of scale deposits

The chemical analyses of scale deposits collected from the separator u-seal, silencer and turbine rotor were carried out using the following two methods in order to determine their structural composition;

X-ray diffraction (XRD analysis) was used to quantitatively analyze the compounds present in the scales deposit and the results were presented as shown in Tables 4.6, 4.8 and 4.10. The procedure for carrying out XRD analysis is detailed in section 2.8.1. An XRD analyzer employs an X-ray beam with an angular configuration to the surface of the sample to identify the compounds present in the sample based on the atomic arrangement and configurations on the surface of the samples. The analyzer is able to produce the quantitative composition of compounds present in the samples.

On the other hand, X-ray florescence (XRF analysis) was used to analyze the elemental composition of deposited materials and the results for the analysis were presented in Tables 4.5, 4.7, 4.9 and Figures 4.1, 4.3 and 4.5. XRD analysis was only limited to quantification of compounds present in the samples. For this study, it was necessary to carry out the elemental analysis to ascertain the chemical composition of the solid deposits, by doing so, it helped in comparing the composition of geothermal fluid to that of the scales deposits so as to ascertain the main cause of the scaling deposition in the steam pipes.

4.5.1 XRF and XRD analysis report for the scale samples collected from the cyclone separator u-seal pit

The samples were initially dried at 105 degrees in preparation for the analysis and the species were recorded as oxides.

Table 4.5: XRF analysis report for the scale deposits` samples

Separator u-seal pit scale deposits` XRF analysis report										
Analysis method: X-ray fluorescence (XRF)										
Species	SiO	Al ₂ O	K ₂	Fe ₂	Na ₂	Ca	SO	Cu	F	
	2	3	O	O	O	O	3	O		
Elemental composition (%)	69	9	4	3	3	2	2	1	1	

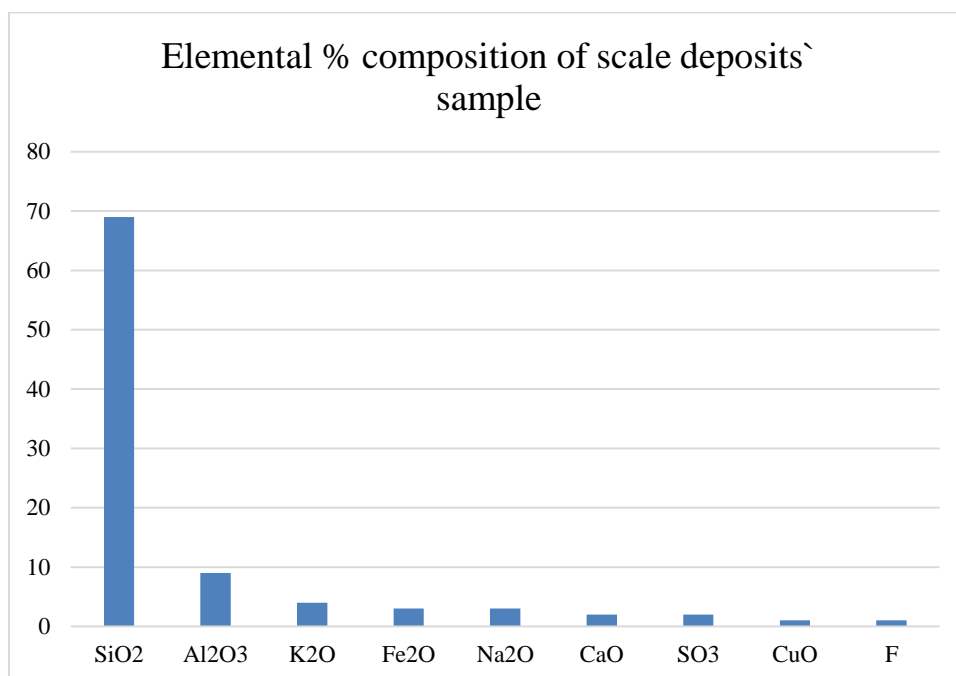


Figure 4. 1: Elemental % composition of scale deposit samples

Table 4. 6: XRD analysis report for scale deposits` samples

XRD report for separator u-seal pit scale deposits` samples	
Compound name	Formula
Silica (silicate)	SiO ₂
Iron Oxide (Magnetite)	Fe ₃ O ₄
Calcium Carbonate (Calcite)	CaCO ₃
Calcium Fluoride (Fluorite)	CaF ₂
Possible compounds	Sodium Aluminium Silicate (Albite)-NaAlSi ₃ O ₈

As indicated in tables 4.5 and figure 4.1, the XRF analysis of the scale samples collected from the cyclone separator u-seal pit showed that, by weight silica (SiO₂) (69%) was the highest composition of the scale deposits followed by aluminium (9%), potassium (4%), iron and sodium at 3% each, calcium and sulphur at 2% each, copper and fluorine at 1% each concluding that the possible dominant compounds was Sodium Aluminium Silicate (Albite)-NaAlSi₃O₈. All these compounds originated from the geothermal fluids in the reservoir. The aim of this analysis was to determine the structural characterization of the scale deposits in the steam pipes. The geothermal fluid being discharged from the well at high pressure and temperature has a high mineral content from the underground reservoir. As the fluid flows up the wellhead and associated pipelines, it boils due to pressure drop, and most solutes are soluble in the brine during this liquid phase. The solubility of silica decreases as the temperature and pressure of the brine drop, becoming much more saturated and gradually precipitating. This continuous temperature and pressure drop allowed the brine to cool, resulting in the deposition of silicon dioxide (silica) and other mineral elements, that is why the scale sample

collected from the Separator u-seal had a high percentage of silicon dioxide-silica. The scale deposit samples collected from this section are shown in figure 4.2.



Figure 4.2: Images of scale samples collected from the separator –u seal pit

4.5.2: XRF and XRD analysis report for scale samples collected from the silencer

The samples were initially dried at 105 degrees in preparation for the analysis and the species were recorded as oxides.

Table 4.7: XRF analysis report for the scale deposits` samples

Silencer scale deposits` XRF analysis report					
Analysis method: X-ray fluorescence (XRF)					
Species	SiO ₂	Na ₂ O	Cl	K ₂ O	SO ₃
Elemental composition (%)	84	4	1	1	1

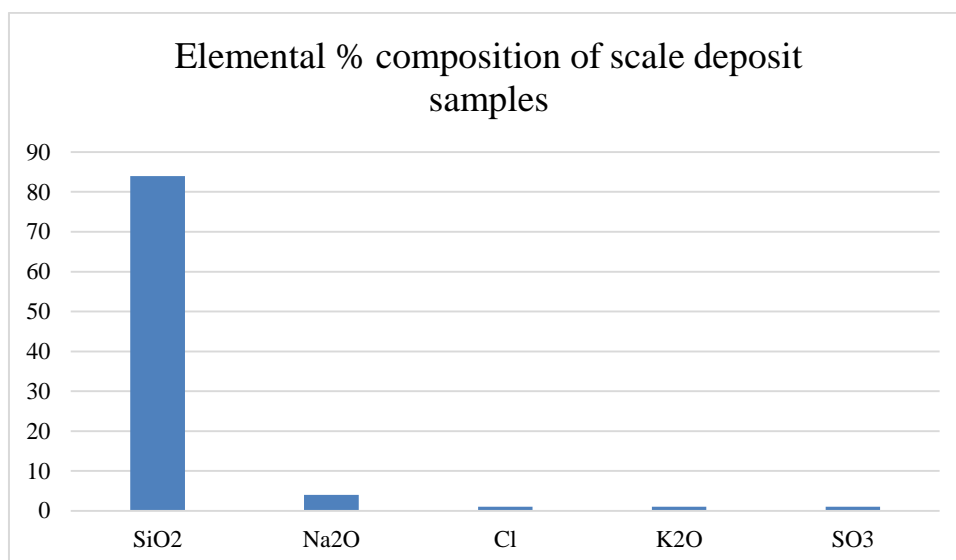


Figure 4.3: Elemental % composition of scale deposit samples

Table 4. 8: XRD analysis report for the scale deposits` samples

XRD report for the silencer scale deposits` sample	
Compound name	Formula
Silica (Silicate)	SiO ₂
Sodium Chloride (Halite)	NaCl
Possible compound	Sodium silicate hydrate magadiite

As indicated in tables 4.7 and figure 4.3, the XRF analysis of scale samples collected from the silencer showed that, by weight silica (SiO₂) (84%) was the highest composition of the scale deposits` followed by sodium (4%) while chloride, potassium and Sulphur at 1% each concluding that the possible dominant compound was sodium silicate hydrate (magadiite). All these compounds originated from the geothermal fluids in the reservoir. The aim of this analysis was to determine the structural characterization of the scale deposits in the steam pipes.

Excess steam and highly mineralized separated brine are directed to the silencer from the separator where it was re-injected back into the production well for further heating (hot re-injection) after the separator extracts dry steam from the brine flowing from the discharge well. The brine had undergone a substantial drop in pressure and temperature at this stage causing silica solubility to decrease and the brine phase to become oversaturated resulting in further cooling and deposition of silicon dioxide (SiO_2) – silica and other dissolved minerals on the silencer. As a result of the high mineral content in the brine from the discharge wells, the scale samples obtained from the silencer contain a high percentage (84%) of silicon dioxide (SiO_2) and other mineral oxides. The scale samples collected from this section are shown in figure 4.4



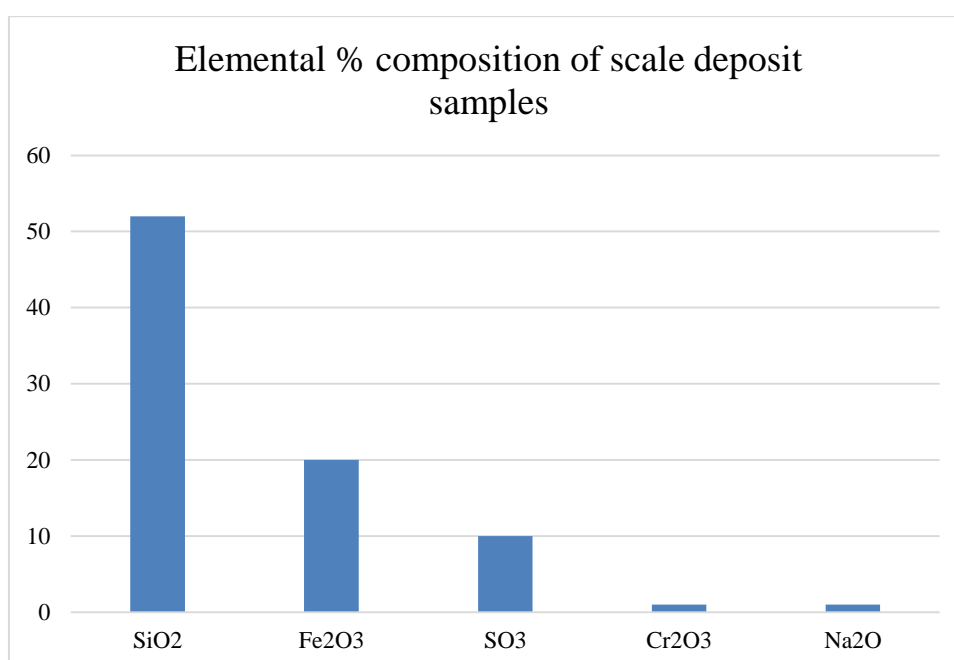
Figure 4. 4: An image of scale sample collected from the silencer

4.5.3 XRF and XRD analysis report for scale samples collected from the turbine exhaust

The samples were initially dried at 105 degrees in preparation for the analysis and the species were recorded as oxides.

Table 4. 9: XRF analysis report for the scale deposits` sample

Turbine exhaust scale deposits` XRF analysis report					
Analysis method: X-ray fluorescence (XRF)					
Species	SiO₂	Fe₂O₃	SO₃	Cr₂O₃	Na₂O
Elemental composition (%)	52	20	10	1	1

**Figure 4.5:** Elemental % composition of scale deposit samples**Table 4. 10:** XRD analysis report for the scale deposits` sample

XRD report for the turbine exhaust scale deposits` sample	
Compound name	Formula
Silica (silicate)	SiO ₂
Iron Oxide (Hematite)	Fe ₂ O ₃
Iron Oxide(Magnetite)	Fe ₃ O ₄
Iron Sulfide (Pyrite)	FeS ₂
Possible compound	Iron silicate

As indicated in table 4.9 and figure 4.5, the XRF analysis of the scale samples collected from the turbine exhaust showed that, by weight silica (SiO_2) (52%) was the highest composition of the scale deposits followed by iron (Fe_2O_3) (20%), Sulphur (10%), chromium and sodium at 1% each concluding that the possible dominant compound was Iron silicate. All these compounds originated from the geothermal fluids in the reservoir. The aim of this analysis was to determine the structural characterization of the scale deposits in the steam pipes

The scale deposit was formed from the reaction of iron-rich impurities in the steam to hydrogen sulphide gas (H_2S). H_2S gas dissolved into steam condensate to form a solution, where it dissociated and became reactive, eventually forming pyrite and pyrrhotite after reaction with iron. Magnetite was formed by dissolution and dissociation of carbon dioxide gas. The source of iron may be from the carryover into the steam pipes during two-phase separation in cyclone separators or from transmission pipelines. It was reported that pyrite is a common hydrothermal mineral in Olkaria east field where it occurs at deeper levels.

Silica (SiO_2) and other mineral ions present in the turbine exhaust are as a result of steam carry-over that is responsible for scales deposition on the turbines and other related components exposed to the steam. This is due to brine droplets carried a long and then gets evaporated on the substratum. This is because sometimes separation of steam from the brine do not occur 100% as anticipated. This is the reason why the quality of steam entering the turbine is routinely checked by collecting steam samples at the strainer for analysis of mineral ions to ensure steam entering the turbine is 100% pure. So when the steam rotates the turbine to generate power, more pressure and temperature drop occurs leading to further cooling which results in the deposition of

these solutes on the turbine rotor and blades hence being the reason for the presence of silica and other mineral elements in the scale sample collected from the turbine rotor. These solutes deposit on the turbine rotor will reduce the number of revolutions per second i.e. reduces the efficiency of the rotation of the turbine blades and consequently, low power output. The scale samples collected from this section are shown in figure 4.6.



Figure 4. 6: An image of scale sample collected from the turbine exhaust

4.6 Chemical analysis for the scaling potential

In water-rock reactions, the computer code WATCH (Bjarnson, 2012) was used. Chemical analyses of sampled water, gas, and steam condensates with pH, temperature and pressure at the point of sampling were conducted. At any desired temperature, the computer code WATCH was capable of calculating pH, aqueous speciation, partial gas pressure, redox potential, ionic strength, chemical equilibria and mass balance equations in order to obtain the fluid composition and distribution of species. The capacity of the samples taken from well 37B in this study scale was measured at selected temperature decrements after adiabatic boiling of the well fluids as the fluids pass from the reservoir to the surface.

4.6.1 Overview of scale deposition

Well 37B encountered very low water flow rates of about 0.5 t/h. In October 2019, the water flow rate ranged from 0.5 t / hr to 0.1 t / h in January 2020. Steam performance from this well decreased to 7.41 t / hr in January 2020 from approximately 45.12 t / hr when the well was connected to the production system in October 2019. The output for well OW-37B over time is shown in table 9 below. (KenGen well reservoir data).

Table 4. 11: Well 37B output between October 2019 and January 2020

Year	Steam [t/hr]	Water [t/hr]	Mass Flow [t/hr]	Enthalpy [Kj/Kg]
2019 October	45.12	0.5	448.12	2743
2019 November	36.8	0.9	37.6	2713
2019 December	8.23	0.3	8.2	2748
2020 January	7.41	0.1	7.4	2766

Between October 2019 and January 2020, indicates a sharp drop in steam production. Scale deposits were observed at the T- link at the well head master valve, within the two-phase line, inside the separator and inside the separated water line, during routine maintenance of the well that was carried out in December 2019. The deposition of scale in the well's transmission steam pipes is most likely to be the cause for the drop in steam in this well. Using the XRD analysis, three scale samples were obtained and analyzed, one from the inside of the separator, the silencer, and the other from the turbine rotor. For both samples, the patterns of the XRD peaks could be recognized and they happened to be located at approximately $23^{\circ} 2\theta$ i.e. on the $2D-\theta$ scale, the XRD run revealed 23 angstrom, which was typical of amorphous silica. Such peaks are typical of pure amorphous silica. According to flow tests while the well was on discharge, a leakage of cooler water from shallow depths trickles into the well, after absorbing the

heat from the steam, the shallow cooler water with a small silica concentration mixes with up flowing fluids with a much greater steam fraction and evaporates, supersaturating the fluid with respect to silica and causing silica to deposit out of solution. Of the three samples from the above three sampling points, the XRD runs are shown in figure 4.7.

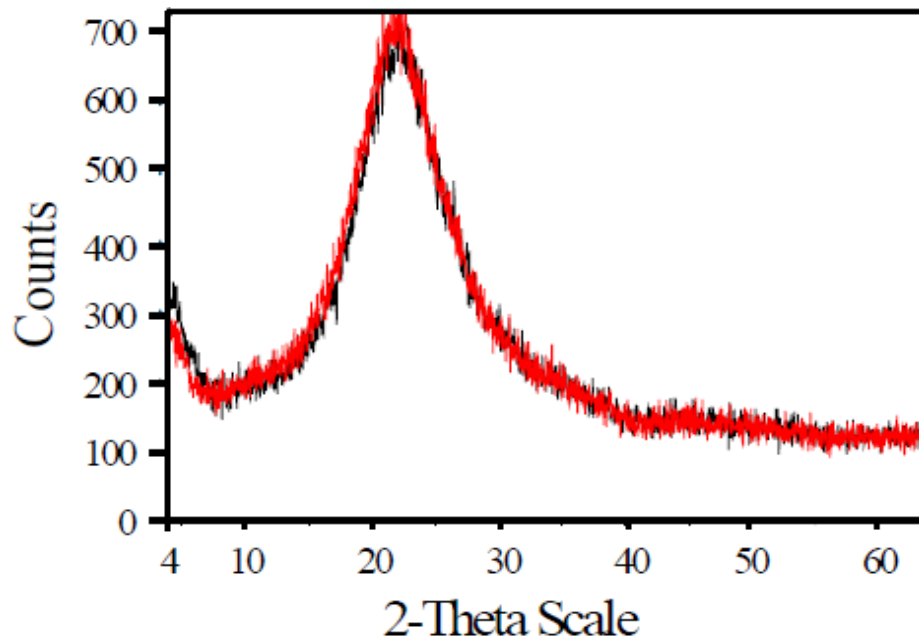


Figure 4.7: XRD peaks for scale samples from the inside of the separator, silencer and from the turbine rotor

As was the case when high concentrations of other electrolytes such as Al^{3+} , Fe^{3+} , Fe^{2+} , Mn^{2+} are present in the brines, the peak is not moved (Gallup, 2013). In this well, scale deposition occurred at various locations and displayed various thicknesses. Measured scale thickness was performed at the T-connection at the master valve of the well head, two-phase line where there was a bend before an orifice, and in the separate water lines. With the help of a vernier caliper, the thickness was measured. Table 4.9 below shows the thickness of scale measurements taken at different positions of the pipeline in this well.

Table 4.12: Thickness of the scale measurements taken at different positions of the steam pipeline

Inside the two-phase fluid pipeline	~ 1 inch
Inside separated water pipeline	~ 0.6 inch
At the wellhead T-connection	~ 0.3 inch

It appears that the highest scale deposition occurred in the two-phase fluid pipeline. In the separated water pipeline, modest deposition occurred, while lower deposition occurred at the T- connection at the wellhead. It is possible that, due to further cooling of the two-phase fluid and further evaporation, most scale deposition occurred in the two-phase fluid pipeline. The scale thickness varying at various positions of the pipeline may have been due to various fluid processes contributing to the creation of the scales. The deposits on the scale and their locations are shown in Figure (4.8- 4.11).

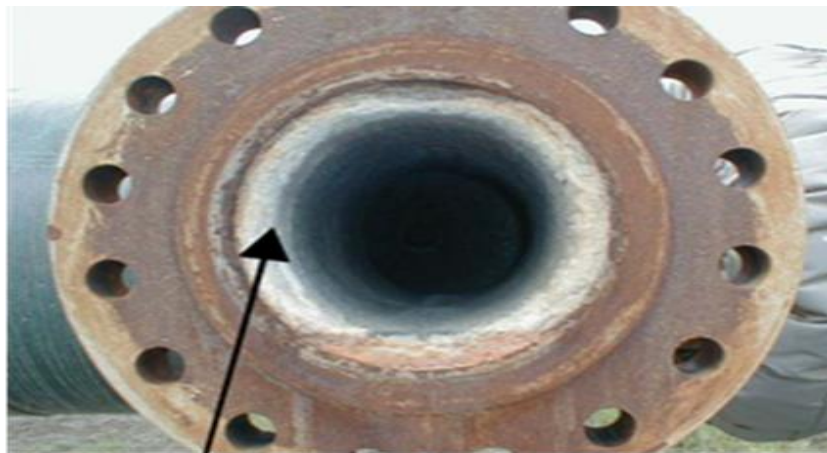


Figure 4.8: Thickness of scale deposited in two-phase fluid pipeline



Figure 4.9: Thickness of scale deposited in separated water pipeline



Figure 4.10: Thickness of scale at the T-Connection of well 37B



Figure 4.11: T-Connection on well 37B

4.6.2 Deposition rate in Well 37B

The deposition rate for silica scaling was calculated from the results in table 4.1 above, as shown in the table 4.10. Much of the amount of silica scaling produced was influenced by the concentration of potential silica deposits within the fluid and the values of the mass flow rate. The higher the possible silica deposit, the larger the rate of deposition. This estimate was achieved by assuming that the brine pipelines were injected with no inhibitor fluid.

Table 4.13: Calculations of deposition rate in well 37B

Well 37B	Location	Potential Deposits	Mass Flow				
			Rate	Deposition Rate			
		mg/kg	Kg/S	ton/hour	ton/day	ton/month	ton/year
	Separator	105		0.0066	0.16	4.8	57.6
			17.4				
	Silencer	620		0.04	0.96	28.8	345.6

Before finalizing the geothermal plant design for a given area, the rate of scale of deposition was very important to understand and probably calculate. It defines the pace of cleaning and the potential need for chemical inhibitors to be used, all of which can be factored into the commercial feasibility of the design for geothermal production.

4.6.3 The solubility of amorphous silica scales

A chemical silica compound [SiO₂] existing in geothermal fluids is present in a variety of mineral forms in the earth sub-surface; quartz, chalcedony, cristobalite, amorphous silica (Brown, 2011a). Quartz is the least soluble of these forms, so it is the equilibrium of quartz solubility that determines the concentration of silica in a geothermal reservoir solution and also in the discharge from geothermal production well. Although this

concentration of saturation depends on a number of variables, temperature predominantly affecting it. The following formula characterizes this dependency (Fournier R. O., 2011):

$$T = -42.196 + 0.28831C - 3.6685 \times 10^{-4} C^2 + 3.1665 \times 10^{-7} C^3 + 77.034 \log C$$

.....4. 1

Where: C is the solution's silica (SiO₂) concentration in mg/kg (ppm).

T is the temperature in degrees °C.

Although quartz solubility controls the concentration of silica in the underground solution, silica is more likely to precipitate inside the process equipment in an amorphous form. It is the balance of amorphous silica solubility that defines the most important saturation concentration in an operational sense. The following formula describes the solubility of amorphous silica and is valid between 0 and 250°C, (Fournier & Rowe, 2010).

$$\text{Log}_{10}[C] = - \frac{731}{(T+273.15)} + 4.52 \dots\dots\dots 4. 2$$

If the concentration of silica in the solution is higher than the concentration described by equation 4.2 at a given temperature, it is likely that a precipitate will be produced at a process environment. Equations 4.1 to 4.2 and the silica supersaturating area are important for the handling of geothermal fluids. The soluble quartz and amorphous concentrations are shown in Figure 4.12.

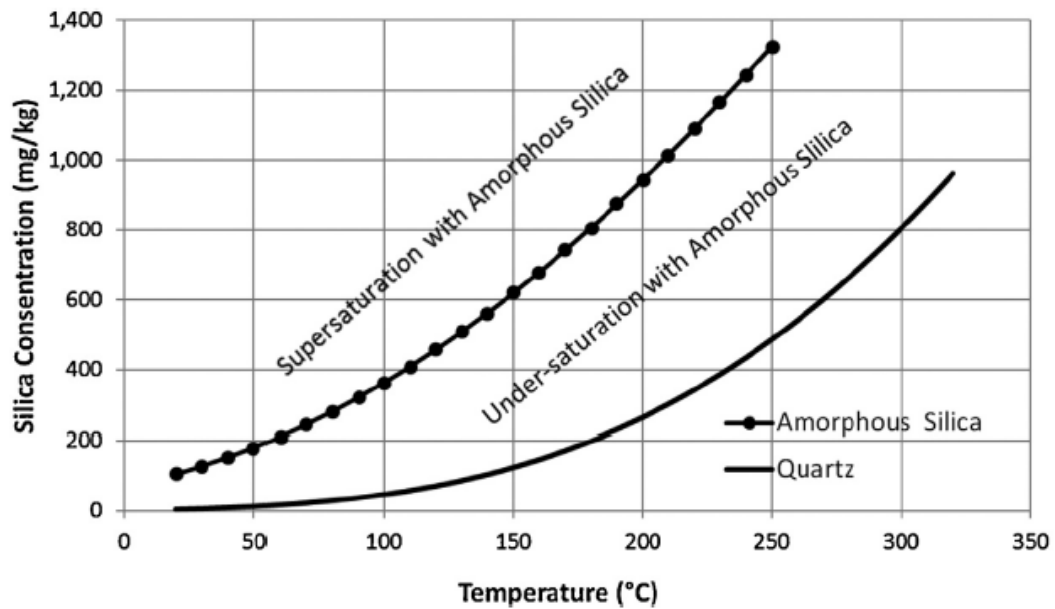


Figure 4.12: Temperature dependence of the solubility of quartz and amorphous forms of silica

It is clear from Figure 4.12 that if the solution temperature drops or the silica concentration of the fluid increases, in a solution saturated with respect to amorphous silica, i.e. on the amorphous silica solubility line, can form precipitates. In steam-field and power station machinery, all of these mechanisms are workable.

When the high-pressure brine is flashed, the concentration of silica in the brine usually increases in separators and flash plants, i.e. releasing it to a lower pressure, then separating steam from the liquid phase. The relative concentration of silica in the remaining solution is increased as silica is not transported with the steam so it stays within the liquid phase. The heat loss and concentration mechanisms can work well at the same time as they actually do in flash separation, but as mechanisms leading to supersaturated conditions, it is worth keeping them conceptually separate.

The degree of saturation of a fluid in a geothermal fluid is basically defined by its silica saturation index (SSI). This is known as the ratio between the measured silica in a solution and the solubility of the amorphous silica at the temperature of the fluid or

brine. Therefore, $SSI > 1$ means that the solution is supersaturated and $SSI < 1$ means that the solution is under-saturated (Brown, 2011a).

4.6.4 The effect of temperature and pH on the deposition of amorphous silica scaling at well 37B

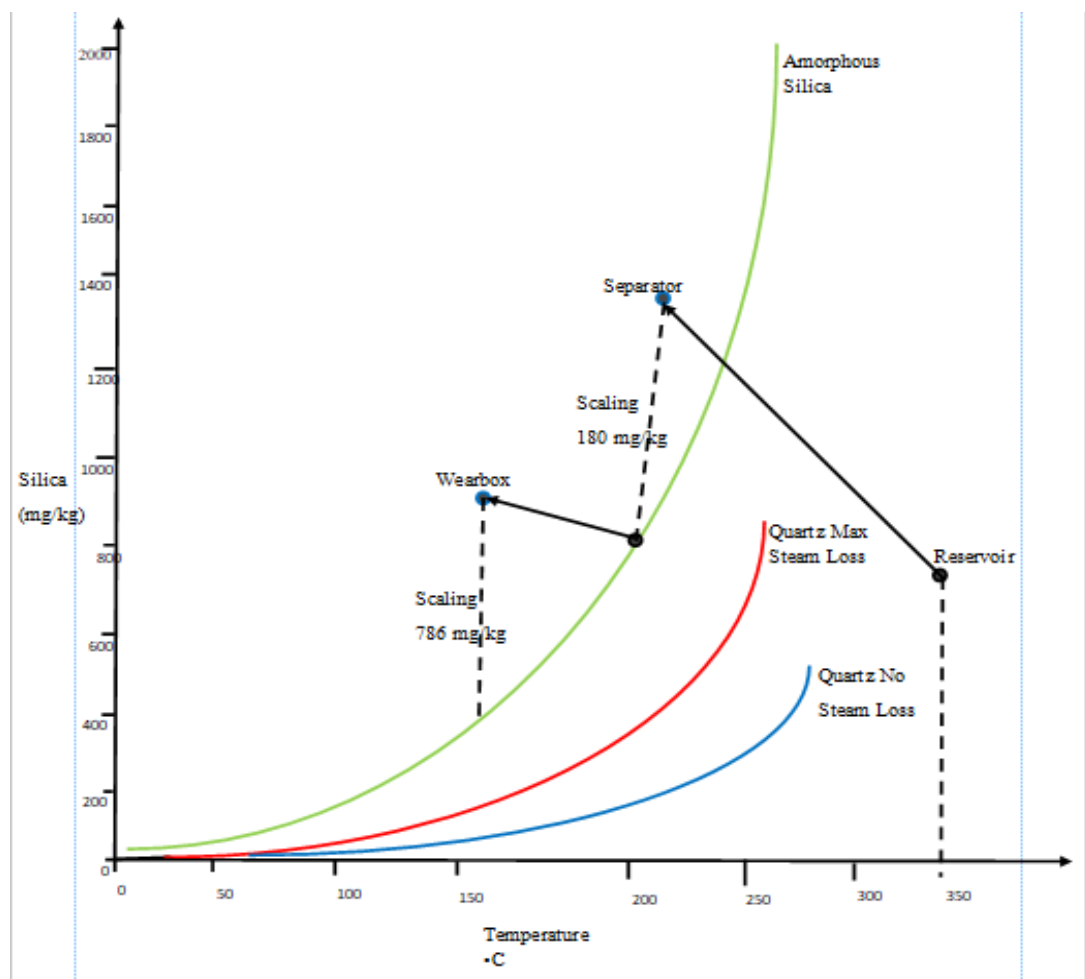


Figure 4.13: The estimated amorphous silica solubility with temperature in well 37B

The water from the reservoir flows adiabatically to the surface through the wellhead. The fluid is then flashed at 7.5 bar or 190°C in the separator. The reservoir's silica concentration is below the amorphous silica saturation curve in Figure 4.13, so no silica scaling occurs. Quartz, cristobalite, and chalcedony do not form in reservoirs because

the fluid flows rapidly at high pressure and temperature. When the fluid enters the separator, the silica concentration will be above the amorphous silica saturation curve, and about 180 mg/kg (SSI: 1.14) of amorphous silica will form before returning to the saturation state. As a result of the steam separation, separated water flows through the brine pipeline from the separator to the weirbox. The water in the weirbox experiences a major change in pressure and temperature, which raises the silica content. Weirbox's silica concentration is also above the amorphous silica saturation curve, with a possible formation of 786 mg/kg (SSI: 2.8).

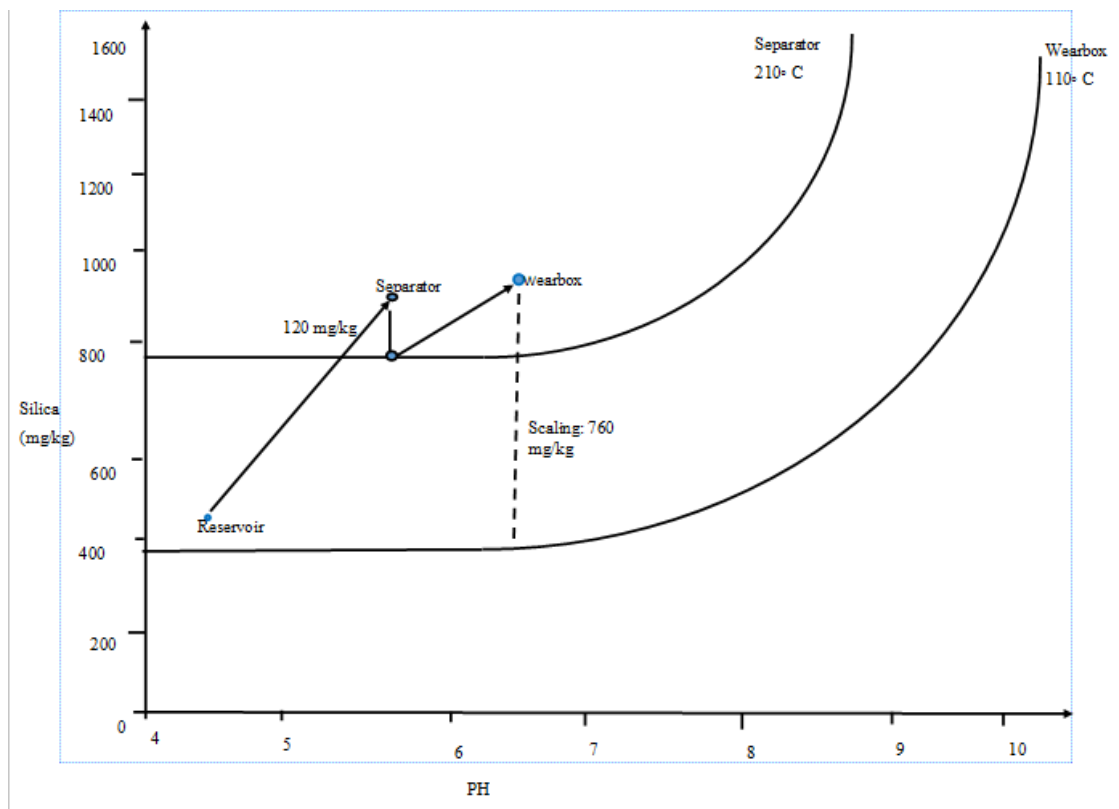


Figure 4.14: The estimated amorphous silica solubility with pH

At about 210°C, the silica concentration within the water in the separator becomes supersaturated in terms of amorphous silica solubility, as shown in Figure 4.14, with pH 6.7. Silica scaling of up to 120 mg/kg could form in the separator before returned to saturation state. The residual water is piped directly to the weirbox, causing the water

to flash at about 110°C. Because of the Carbon (IV) oxide release, the silica concentration becomes more supersaturated over amorphous silica solubility, and the water pH rises (pH 7.5). In addition, about 760 mg/kg of silica scaling is formed.

4.6.5 Effects of amorphous silica scaling on pressure drop

All steam pipe flows are subject to frictional losses; pressure drops as a consequence of fluid or conduit boundary interactions and fluid turbulence due to energy lost. This mechanism of energy loss depends on flow properties such as fluid viscosity, conduit shape and size, and flow velocity. In addition, the roughness of the steam pipe is one of the key reasons for this kind of energy loss. Darcy Weisbach's equation commonly expresses this association between pressure drop, flow characteristics and roughness in a circular pipe:

$$\Delta p = f \cdot \frac{L}{D} \cdot \frac{\rho v^2}{2} \dots\dots\dots 4.3$$

where; Δp is pressure drop in Pascal, f a dimensionless friction factor, L and D are length and internal diameter of the pipe (m) respectively, ρ is the fluid density (kg/m^3) and V is the average fluid velocity (m/s).

In this formula, the dimensionless friction factor (f) is in turn a function of two other quantities; the relative roughness ϵ/D where ϵ is the pipe wall average roughness height with internal diameter D and the Reynold`s number. The Reynold`s number (Re) is the ratio of inertia to viscous forces, defined as:

$$Re = \mu VD / \rho \dots\dots\dots 4.4$$

Where: μ is fluid viscosity measured in Pascal seconds.

The exact correlation between roughness, the Reynold`s number and the friction factor is formulated both implicitly (Moody & Princeton, 2012) and explicitly in a number of different ways, all of which aim to reflect findings found in broad empirical data groups. Such a formulation of the relationship between fluid flow, pipe roughness and friction factor is described by the Haaland equation (Munson, Young, & Okiishi, 2009).

$$\frac{1}{\sqrt{f}} = - 1.8 \log_{10} \left[\left(\frac{\varepsilon/D}{3.7} \right)^{1.11} + \frac{6.9}{Re} \right] \dots\dots\dots 4. 5$$

Equation 4.5 has the advantage of having an explicit formulation for the friction factor.

Shock losses are another cause of the pressure drop in the piping systems. There are pressure drops due to sudden changes in the direction of fluid flow, such as bends, valves and other pipe fittings. Lower loss coefficients are used in order to account for these types of pressure losses, in which it is presumed that the pressure drop from a fitting is proportional to the dynamic flow pressure, i.e.

$$\Delta p \propto \frac{\rho v^2}{2} \text{ or } \Delta p = k \cdot \frac{\rho v^2}{2} \dots\dots\dots 4. 6$$

Where: k is the minor loss coefficient.

By assuming that there will be shock losses at the entrances to the steam pipes and at the entrance and exit of each steam pipe, this type of loss was included in the friction factor or relative roughness calculations. Even with these easy connections, the effect of scaling on the friction factor and pressure drop can be complicated. Secondly, scaling will result in a flow cross section restriction that will increase the fluid velocity for the same mass flow. This increases the volume, height of roughness and friction factor of the Reynold`s number. At the same time, the pressure drop is inversely proportional to the hydraulic diameter, equation 4.4 and as the flow conduit restricts, the total pressure

drop will increase. Alternatively, scaling may be rough and increases the friction factor or may not be rougher than the original wall of the pipe (Bott, 2009). These parameters would eventually interact, making it very difficult to estimate the impact of scaling on output a priori and highly dependent on the assumptions made about the manner of deposition of the scale. These problems underscore the need for a good understanding of the parameters influencing the rate of silica scaling and morphology on a case-by-case basis, even for the same operation.

(Bott, 2009) Confirmed that there appears to be asymptotic scaling due to silica in geothermal steam pipes. Experimental experience has shown that resistance to scaling is negative for the number of Reynolds in the range of 23,000-44,000. This is due to the roughness of the silica deposits compared to clean smooth steam pipes, which improves the heat transfer. The silica deposit induces ripple formation, i.e. increased turbulence that increases the coefficient of heat transfer near the internal surface. However, one must note that continuous thick scaling build-up can serve as an insulator or reduce the velocity of fluid flow significantly. This can result in the heat transfer coefficient being effectively reduced. It can completely block the steam pipes and other geothermal equipment in the worst-case scenario.

4.7 Effect of Amorphous Silica Scales Deposition on the Turbine and Plant Power Output

4.7.1 Decline of well 37B power output

Decline of well output: recently, the output of well 37B, which had a high enthalpy at first, had drastically decreased (table 4.11). The following were some of the possible explanations:

- i. Plugging due to amorphous silica deposition in the well
- ii. Casing damage
- iii. Decline of reservoir pressure (capacity)

Table 4.14: Wellhead pressure drop of well 37B after several months of production

Description	October	November	December	January
	2019	2019	2019	2020
Initial pressure (bar)	11.5	7.3	12.6	9.3
Pressure at present (bar)	5.0	3.2	6.4	3.7

There were indications of amorphous silica deposition observed in wellhead equipment and other plant facilities. Scale samples had been taken from the surface equipment of this well and on the ground where wastewater is discharged from the surface. Specifically, at the bottom of the wellhead separator, scale deposits were found. Additionally, the brine line valves were difficult to open and close, which could be due to amorphous scaling. From the chemical analysis of the geothermal fluid, the scaling potential was assessed using WATCH program. The results showed a great possibility of amorphous scaling. This amorphous scaling problem is presently causing operational challenges at the geothermal power plants.

Therefore, it was possible to conclude that;

- i. A possible case for decline in well 37B output was due to amorphous silica deposition. Running buckets of different diameters into the well was required to clear scale obstructions in the well bore.
- ii. Another cause was pressure drawdown and decline in enthalpy (temperature / heat content of the fluids). Monitoring of the downhole pressure and temperature logs was required to ascertain reservoir behavior.

Utilization of a geothermal resource involves extracting mass and heat (dry steam) from the fluid to drive a turbine which in turn drives an electric generator to produce electricity. It is through the turbine nozzles that fluid enthalpy is converted to kinetic energy that drives the turbine. The mechanical energy developed by the turbine is converted into electricity by direct coupling to an electric generator. The turbine output of the plant is measured by the amount of enthalpy change of the fluid. In liquid dominated high temperature geothermal fields, amorphous scale deposition is a problem for steam turbines. Deposition of amorphous silica scales take place mainly in turbine inlet nozzles and slightly on the rotating turbine blades. Only small deposition can be found on the first stage of turbine blades. This results in the loss of power output due to restrictions of the steam flow.

The turbine's output is a direct function of mass flow rate and enthalpy change. The output power is expressed as;

$$P = m (h_i - h_o) \eta_t \eta_g \dots\dots\dots 4.7$$

Where; P = Power generated (kW)

M = Mass flow rate (Kg/S)

h_i = Enthalpy at turbine inlet pressure (KJ/Kg)

h_o = Enthalpy at turbine outlet pressure (KJ/Kg)

$\eta_t \eta_g$ = Turbine and generator efficiencies

Amorphous silica scaling narrows the throat of turbine nozzles and as result decreases the amount of steam flow into the turbine. Therefore, the power output which is highly dependent on the steam mass flow declines as restricted mass flow rate passes through

the turbine blades. To utilize geothermal fluid at maximum efficiency, the purity and quality of the dry steam must be maintained.

4.7.2 Effects of amorphous silica scales on the turbine output

Amorphous silica scales have previously deposited on turbine nozzles over time, limiting the steam flow, resulting in turbine inlet and steam chest pressure increase from 4.0 to 4.5 bar and from 3.5 bar to more than 4.0 bar respectively as shown in Table 4.15. This was assumed to be the main cause of low turbine output that was slightly above 34 MWe. After cleaning the shroud manually by removing the deposits, the turbine load, steam chest pressure, and steam inlet pressure all improved dramatically as the power output increased from 34 to 37 MWe.

Deposition of total dissolved solids, silica and other solutes contained in the steam carryover on the turbine reduces the number of revolutions per second of the blades, lowering the efficiency of the turbine blades rotation and, as a result, lowering the power output of the plant.

Table 4.15: Effects of amorphous silica scales on the turbine output

	Original pressure (bar)	Pressure at present (bar)
Turbine inlet pressure	4.0	4.5
Steam chest pressure	3.5	4.0

The condensers equipment can suffer from amorphous silica deposition on the brine distribution plates. This results in the loss of power and vacuum. So, for a condensing turbine, a clean condenser is critical for maximum power output. As condensers are part of the power making equipment, they have to be clean all the time for efficient cooling. Similarly, amorphous silica deposits can plug the brine distribution nozzles on top of a

cooling tower, severely affecting brine distribution over the tower fills, and thus badly influencing the cooling tower performance.

Amorphous silica scales are substantially deposited in brine fluid pipes. Build-up of amorphous silica deposits in drains and the pipe carrying residual geothermal brine from different pipe lines has been a challenging problem in geothermal power plants globally.

CHAPTER FIVE

CONCLUSIONS AND RECOMMENDATIONS

5.1 Conclusions

Analysis of the geothermal fluid samples collected at different points of the power plant showed the characteristics of the fluids in terms of silica (SiO_2), pH, total dissolved solids (TDS), conductivity, Sulphates, enthalpy and Cations (Iron and Sodium). The composition of the geothermal fluids as they flow into the separator chamber, dry steam entering into the turbine, condensates leaving the turbine exhaust and separated water going into the silencer, the characterization of the scale deposits at the cyclone separator U-seal pit, turbine rotor (exhaust) and the scale compositions at the silencer were all important factors in determining the conditions favoring deposition of amorphous silica scales in well 37B in Olkaria power plant.

According to the findings of the research, it was concluded that the major cause of the deposition of amorphous silica scales on the plant and equipment's in well 37B were:

- i. Deposition of amorphous silica scales occurred due to the geothermal fluids pressure drop, temperature and pH changes. It was found that pH decrease was the principal cause of amorphous silica scaling deposition while temperature decrease was the more significant cause of scaling in steam pipes and equipment's.
- ii. The deposits on the turbine blades were mostly made up of pyrite (FeS_2), magnetite (Fe_3O_4), and iron oxides, which were formed when iron and hydrogen sulphide or carbon dioxide fumes reacted with water to generate pyrite (FeS_2), magnetite (Fe_3O_4), and iron oxides. The iron may come from deep within the

reservoir or from mild steel steam lines, and it could enter steam pipelines via brine carry-over.

5.2 Recommendations

The research has identified the root cause of the amorphous silica scales deposition in the steam pipes and plant equipment's being geothermal fluids pressure drop, temperature and pH changes where pH decrease was the principal cause of amorphous silica scaling deposition while temperature decrease was the more significant cause of scaling. This research therefore recommends the following:

- i. An alternative method of pH modification in geothermal plants was explored which was dilution of the separated brine with steam condensates that involves mixing steam condensates with separated brine in specified fractions to help raise the pH of the resultant mixture and keep the temperatures above the amorphous silica saturation temperature to avoid scale deposition in steam pipelines and equipment. The steam condensates are mixed with the separated brine from the wells in the production fields, rather than being neutralized with sodium carbonate (Na_2CO_3) as is currently done in Olkaria. The separated brine from the Olkaria fields is highly alkaline with a pH of above 9.0 and temperatures of above 150°C . The steam condensates on the other hand is at the pH of about 2.5 and temperature of above 50°C .

This approach evaluates the scaling potential before and after mixing the fluids, as well as how the pH changes when mixing the steam condensates and separated brine in various mixing ratios ranging from 90% condensates and 10% brine to 50%

condensates and 50% brine. More condensates to brine is taken because the aim is to increase the pH of the condensates.

This can be done using PHREEQC which is a geochemical modelling software code, and WATCH. The PHREEQC software simulates the mixing of different fluids while determining the scaling potential of amorphous silica. According to the findings, mixing the steam condensates from power plant with the separated brine reduces the amorphous silica scaling potential in the plant equipment's and also raises the pH of the fluid.

The major risk with neutralizing the acidic steam condensates with sodium carbonate (Na_2CO_3) as currently done in Olkaria to raise the geothermal fluid pH is the side reactions from the impurities in the chemical such as sulphides and silicates. Implementing this approach will also save the company millions of money spent in purchasing sodium carbonate (Na_2CO_3).

- ii. Dispose of spent high-temperature water (steam condensates) at temperatures above amorphous silica saturation (say, above 100°C for Olkaria wells), by re-injecting it back into the wells.
- iii. To prevent sulphur deposition, the pH of recirculating water from the cooling tower to the condenser must be kept between 6.5 and 8.0. The pH in the current plant operation is unpredictable due to inconsistencies in soda ash dosing or inaccurate instrument readings.
- iv. Steam scrubbing should be employed to clean the steam. In this process, condensate is fed into the steam pipelines on the upstream of a steam scrubber. After that, the condensate is drained from the scrubber. In addition, the

conductivity of steam must be closely monitored in order to keep track of the concentration of solutes in relation to steam wetness.

- v. Further studies need to be carried out on the viability of mixing the separated brine with steam condensates to raise the pH to mitigate deposition of amorphous silica scales on the plant equipment's and in reinjection wells in the Olkaria fields.

5.3 Contributions to new knowledge from this research work

The findings of this research will go a long way to add on to the already existing knowledge base, to take efficiency, durability, and utilization of steam pipes in geothermal power plants to the next level. This research has also contributed some new information useful to the management at Olkaria geothermal fields, to enhance efficiency in the daily operations so as to maximize returns from the project.

REFERENCES

- Armannsson, H., & Hardardóttir, V. (2010). Geochemical patterns in saline high temperature geothermal systems. In Birkle, P. and Torres-Alvarado, I.S (editors), *water-rock interaction. CRC press, Taylor and Francis Group London, 133-136.*
- Arnorsson, S. (2010). *2000a: The quartz and Na/K geothermometers. I. New thermodynamic calibration. Proc. of World Geothermal Congress. Kyushu-Tohoku, Japan.*
- Arnorsson. (2013). Deposition of calcium carbonate from geothermal waters-theoretical considerations. *Geothermics, 18, 33-89.*
- Arnorsson, S. (2010). Gas Chemistry of Volcanic Geothermal Systems. *Proceedings World Geothermal Congress. Bali, Indonesia.*
- Arnorsson, S., & Stefansson, A. (2012, April). Wet-steam well discharges. 1. Sampling and calculation of total discharge compositions. *In proceedings World Geothermal Congress, 24-29, paper 0870. Antalya, Turkey.*
- Arnorsson, S., & Stefansson, A. (2013). Fluid-fluid interactions in geothermal systems. *Rev Mineral Geochem, 259-312.*
- Arnorsson, S., D'Amore, F., & Gerardo-Abaya, J. (2000). Isotopic and Geochemical Techniques in Geothermal Exploration, Development and use: Sampling Methods, Data Handling, Interpretation (ed. Arnorsson, S), International Atomic Energy Agency publication, Vienna.
- Axelsson, G., & Gunnlaugsson, E. (2010). Long-term monitoring of high-and low-enthalpy fields under exploitation. *World Geothermal Congress 2000, pre-congress course. Kokonoe, Japan.*
- Barbier, E. (2012). Geothermal Energy Technology and Current Status. *Renewable Energy and Sustainable Energy Review, pp. 3-65.*
- Barnett, P. R., & Garcia, S. E. (2010). Approaches to controlling silica deposition in geothermal production operations. *Proceedings 15th New Zealand Geothermal Workshop, 1993, University of Auckland, New Zealand.*
- Bergna, H. E., & Roberts, W. O. (2010). Colloidal silica. *Fundamentals and applications. Boca Raton, FL: Taylor & Francis Group.*
- Bjarnson, J. O. (2012). The speciation programme WATCH, version 2.1 Orkustofnun, Reykjavik, 7pp.
- Bott, T. R. (1995). Fouling of Heat Exchangers. Elsevier science, ISBN 0-444-82186-4.
- Brown, K. L. (2010). Test rig experiments for silica scaling inhibition. In: Proceedings of the World Geothermal Congress, Bali, Indonesia, pp. 25-29.

- Brown, K. L. (2011). PH control of silica scaling. *Geothermal Workshop, Vol 5, 157-162*.
- Brown, K. L. (2011a). Thermodynamics and kinetics of silica scaling. In: Proceedings International Workshop on Mineral Scaling, Manila, Philippines.
- Burton, A., Bourcier, A., Burton, C., & Leif, R. (2013). Silica scale management: Lowering operating costs through improved scale control, and adding value by extracting marketable by-products. *Geothermal Resources Council Transactions, 27,519-522*.
- Chen, C. T., & Marshall, W. L. (2013). Amorphous silica solubilities IV. Behaviour in pure water and aqueous sodium chloride, sodium sulphate, magnesium chloride and magnesium sulphate solutions upto 350°C. *Geochim. Cosmochim. Acta,46, 279-288*.
- Corsi, R. (2011). Corrosion and scaling in geothermal fluids. *Geothermics,15, 94-96*.
- Criaud, A., & Fouillac, C. (2013). Sulfide scaling in low-enthalpy geothermal environments: A review *Geothermics. 73-81*.
- E. A., & M. W. (1977). *Chemistry and geothermal systems. Academic Press, New York, 399 pp*.
- Erlindo, C. (2011). *An experiment on monomeric and polymeric silica precipitation rates from supersaturated solutions. Report 5 in: Geothermal Training in Iceland 2006. UNU-GTP, Iceland,.*
- Fournier, R. O. (2011). In: Berger, Bethke (Eds.), *Reviews in Economic Geology Volume 2. Geology and Geochemistry of Epithermal Systems Society of Economic Geologists, pp. 46-61*.
- Fournier, R. O. (2012). The behaviour of silica in hydrothermal solutions.in.Berger, B.R and Bethte, P.M (eds). *Geology and geochemistry of epithermal systems. Society of Economic Geologists. 45-61*.
- Fournier, R. O. (2013). A method of calculating quartz solubilities in aqueous sodium chloride solutions. *Geochim.Cosmochin.Actas, 47, 579-586*.
- Fournier, R. O., & Marshall, W. L. (2011). Calculation of amorphous silica solubilities at 25°C to 300°C and apparent cation hydration numbers in aqueous salts solutions using the concept of effective density of water. *Geochim.Cosmochim.Actas,47, 587-596*.
- Fournier, R. O., & Potter, R. W. (n.d.). The solubility of quartz from 25° C to 900° C at pressures upto 10,000 bars. *Geochim. Cosmochin.ACTas,46, 1966-1973*.
- Fournier, R. O., & Rowe, J. J. (1966). Estimating of Underground Temperature From Silica Content of Water From Hot Springs and Wet Steam Wells, *Am.J. Sci, 264,pp.685-697*.

- Fournier, R. O., & Rowe, J. J. (2010). The solubility of amorphous silica in water at high temperatures and pressures. *Am. Mineral.* 62, 1052-1056.
- Fournier, R. O., & Rowe, J. J. (2012). Estimation of underground temperatures from the silica contents of water from hot springs and wet steam wells. *Am.J.Sci.*, 264, 685-697.
- Fridleifsson, I. B. (2011). Geothermal energy amongst the world's energy sources. *Proceedings of World Geothermal Congress 2005.*
- Gallup, D. L. (2013). Aluminium silicate scale formation and inhibition (2): scale solubilities and laboratory and field inhibition tests. *Geothermics*, 27, 485-501.
- Giggenbach, W. F. (2012). Chemical techniques in geothermal exploration. In: D'Amore, F. (Coordinator), *Application of geochemistry in geothermal reservoir development.* UNITAR/UNDP publication, Rome, 119-142.
- Giggenbach, W., & G.R. (2011). *Methods of Collection and Analysis of Geothermal and Volcanic Water and Gas Samples.* New Zealand Department of Scientific and Industrial Research Report.
- Giroud, N. (2012). A chemical study of arsenic, boron and gases in high-temperature geothermal fluids in Iceland. *Dissertation for the Degree of Doctor of Philosophy, University of Iceland.*
- Gunnarson, I., Ivarsson, G., Sigfusson, B., Thrastarson, E., & Gislason, G. (2010). Reducing silica deposition potential in waste water from Nesjavellir and Hellisheidi power plants, Iceland. *Proceedings World Geothermal Congress 2010, Bali, Indonesia*, 5pp.
- Gunnarsson, I., Arnorsson, S., & Jakobsson, S. (2015). Precipitation of poorly crystalline antigorite under hydrothermal conditions. University of Iceland, Institute of Earth Sciences, 15pp.
- Henley, R. W. (1983). *PH and silica scaling control in geothermal field development.* *Geothermics* 12, 307-321.
- Hirowatari, K., & Yamauchi, M. (2012). Experimental study on scale prevention method using exhausted gases from geothermal power station. *Geoth.Res.Council, Transactions*, 14, 1599-1602.
- Holm, Alison, Dan, Jennejohn, & Leslie Blodgett. (2012). Geothermal Energy and Greenhouse Gas Emissions. *Washington DC: Geothermal Energy Association.*
- Hurtado, R., Andritsos, N., Mouza, A., Mitrakas, M., Vrouzi, F., & Christanis, K. (2010). Characteristics of scales from Milos geothermal plant. *Geothermics*, 18,, 169-174.
- Karingithi. (2010). Processes controlling aquifer fluid composition in the Olkaria geothermal system, Kenya. *Journal of Volcanology Geothermal Resource*, 57-76.

- Karingithi, C. W., & Opondo, K. M. (2011). Hydrothermal mineral buffers controlling reactive gas concentrations in Olkaria geothermal system, Kenya. *Geochim.Cosmochim.Acta.submitted*.
- KenGen. (2011). Surface exploration of Kenya`s geothermal resources in the Kenya Rift. *The Kenya Electricity Generating Company, Ltd, internal report, 84 pp*.
- Kristmannsdottir, H., & Sirgurgeirsson, M. (2010). Sulphur gas emissions from geothermal power plants in Iceland. *Geothermics, 29, 525-538*.
- Mahon, W. J. (2010). Silica in hot water discharge from drillholes at Wairakei, New Zealand. *New Zealand Jour. Sci,9, 135-144, 135-144*.
- Malimo, S. J. (2013). Fluid Chemistry of Menengai Geothermal wells, Kenya. *Geothermal Resources Council Transactions, 56-62*.
- Manceau, A., Ildephous, P. H., Hazermann, J. L., Flank, A. M., & Gallup, D. (2011). Crystal chemistry of hydrous iron silicate scale deposits at the Salton Sea geothermal field, Clays and clay minerals 43, 304-317.
- Marshall, W. L., & Warakowski, M. J. (2014). Amorphous silica solubilities-II. Effects of aqueous salt solutions at 25°C. *Geochim. Cosmochim.Acta, 46, 289-291*.
- Mecardo, S., & Hurtado, R. (2011). Scale incidence on production pipes of Cerro geothermal wells. *Geothermics,18,225-232*.
- Meier, M. (2001). Material Science Central Facilities Department of Chemical Engineering. University of Carlifornia, Davis.
- Molina, A. (2012). Rehabilitation of geothermal wells with scaling problems. *Report 9: Geothermal training in Iceland, 207-240. (UNU G.T.P, compiler)*.
- Moody, L. F., & Princeton, N. J. (2012). *Friction factors for pipeflow. Trans.ASME 8, 671-684*.
- Munson, B. R., Young, D. F., & Okiishi, T. H. (2009). *Fundamentals of fluid mechanics*.
- Omenda, P. A. (2010). Anactetic origin for Comendite in Olkaria geothermalfield, Kenya Rift; Geochemical evidence for syenitic protholith. *African Journal of Science and Technology., 39-47*.
- Opondo. (2010). Fluid characteristics of three exploration wells drilled at Olkaria Domes field, Kenya. *Proceedings of 33rd Workshop on Geothermal Reservoir Engineering, 6. Carlifornia: Stanford University*.
- Opondo, K. M., & Ofwona, C. O. (2013). Investigations of unusual scale deposition in Olkaria well OW-34. *KenGen, Nairobi, unpublished internal report, 11 pp*.
- Ormat. (2011). The power of innovation, projects, geothermal power plants: Ethiopia, Aluto-Langano.

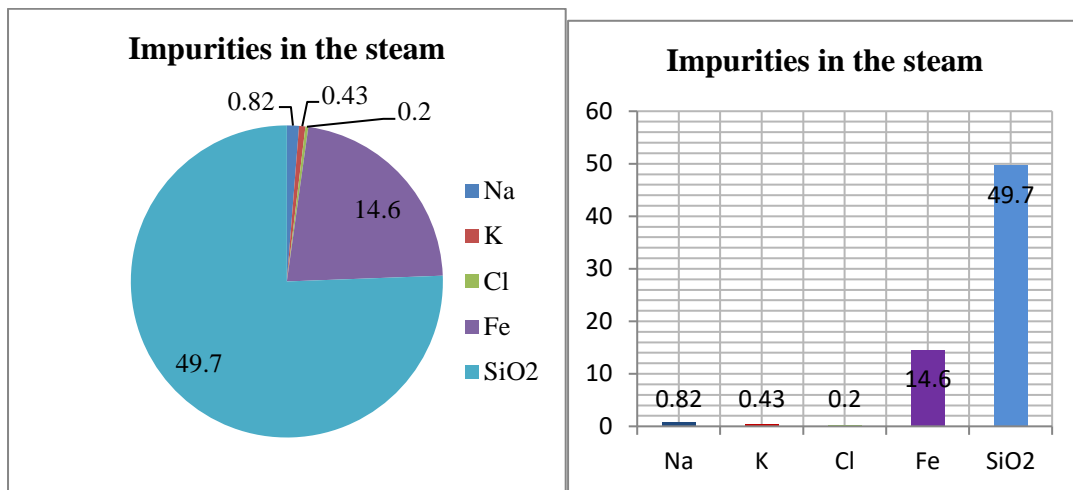
- Oskarsson, F. (2019). Geothermal sampling and analysis. UNU-GTP short course IV on Exploration and Development of Geothermal Resources. Lake Naivasha and Bogoria. 10.
- Otieno, V. O., & Kubai, R. (2013). *Borehole geology and hydrothermal mineralisation of well - 37A, Olkaria East Geothermal field, Kenya. Report 2 in: Geothermal Training Programme in Iceland, 2013. UNU - GTP, Iceland, 105 pp.*
- Pieri, S., Sabatelli, F., & Tarquini, B. (2011). Field testing results of downhole scale inhibitor injection. *Geothermics, 18, 249-257.*
- Pieri, S., Sabatelli, F., & Tarquini, B. (2013). Field testing results of downhole scale inhibitor injection. *Geothermics, 18, 249-257.*
- Simmons, S., & Christenson, B. W. (2012). Towards a unified theory on calcite formation in boiling geothermal systems. *Proc. of 15th New Zealand Geothermal Workshop, Auckland, 145-148.*
- Sinclair, L. (2012). *Development of Silica Scaling, Test Rig.* University of Canterbury.
- Sinclair, L. (2012). *Development of Silica Scaling, Test Rig: University of Canterbury.*
- Solis, P. R. (2010). Calcite deposition in two phase lines of Bacman on Geothermal production field, Phillipines. *Proc. of World Geothermal Congress 2000, Kyushu-Toshuku, Japan.*
- Tassew, M. (2001). Effect of Solid Deposition on Geothermal Utilization. . *Geothermal Training Programme. The United Nations University.* Reykjavik, Iceland.
- Thorhallsson, S. (2012). Common problems faced in geothermal generation and how to deal with them. Presented at short course on Geothermal Development and Geothermal wells, organized by UNU-GTP and LaGeo, in Santa Tecla, El Salvador., 14 pp.
- Villasenor, L. B. (2011). Silica scaling in Tiwi - current solutions. *International Workshop on Mineral Scaling.* Manilla, Philippines.
- Vogel. (2013). *Standard methods for the examination of Water and Waste water.* American Public Health Association.
- Wambugu, J. M. (2011). *Assessment of Olkaria - Northeast geothermal reservoir, Kenya based on well discharge chemistry. Report 20 in: Geothermal Training in Iceland 1996 UNU-GTP, Iceland, 481 - 509.*
- Were, O., & Tsao, L. (2010). Chemistry and Silica in Cerro Prieto brines. *Geothermics, 10. 255-276.*
- Yakoyama, T., Takahashi, Y., Yamanaka, C., & Tarutani. (2011). Effect of aluminium on the polymerization of silicic acid in aqueous solution and the deposition of silica. *Geothermics, 18, 321-326.*

APPENDICES

Appendix A: Data for Brine and Scales Samples Analysis

Physical and chemical composition of brine samples before steam extraction at the separator. Elements are reported as ions

Well 37B	20/02/2020	21/02/2020	22/02/2020
WHP (Barg)	7.5	7.75	7.5
GSP (Barg)	7.5	7.5	6.5
Discharge Enthalpy (KJ/Kg)	2449	2407	2363
Mass flow Rate (Kg/S)	21.6	15.2	15.4
TDS (ppm)	1140	1080	1200
pH@22 ° C	8.33	8.33	8.7
B ⁻ (ppm)	1.71	1.35	1.13
SO ₄ ²⁻ (ppm)	380.95	351.93	338.6
Cl ⁻ (ppm)	474.55	510.23	850
Fe ²⁺ (ppm)	40.53	41.98	61.06
Silica (SiO ₂ ⁻) ppm	769	708	882
Ca ²⁺ (ppm)	1.437	1.691	5.662
Li ⁺ (ppm)	1.71	1.677	1.669
Na ⁺ (ppm)	453	426.3	510
K ⁺ (ppm)	66.86	69.07	84.89
Mg ²⁺ (ppm)	0.426	0.583	0.301
CO ₂ (mmoles/100moles of H ₂ O)	429.4	346.2	362
H ₂ S (mmoles/100moles of H ₂ O)	12.63	10.77	10.08
CH ₄ (mmoles/100moles of H ₂ O)	1.49	1.42	0.75
H ₂ (mmoles/100moles of H ₂ O)	17.43	17.1	13.91
N ₂ (mmoles/100moles of H ₂ O)	79.92	76.41	56.57
Conductivity (µs)	2930	2911	2899

Appendix B: Steam impurities at the turbine inlet

Appendix C: XRF and XRD analysis report for scale samples collected from the cyclone separator u-seal pit

Sampling date: 23/02/2020	
Appearance	
Condition of Solids: Grey	Physical state: Deposit
Color of Sample: Black	
Elemental Analysis by X-ray Fluorescence	
<i>The sample preparation was: Dried at 105 degrees</i>	
<i>The results are reported as oxides.</i>	
Silica (SiO ₂)	69 wt%
Aluminium (Al ₂ O ₃)	9 wt%
Potassium (K ₂ O)	4 wt%
Iron (Fe ₂ O ₃)	3 wt%
Sodium (Na ₂ O)	3 wt%
Calcium (CaO)	2 wt%
Sulfur (SO ₃)	2 wt%
Copper (CuO)	1 wt%
Fluorine (F)	1 wt%
Analysis by X-Ray Diffraction	
<i>The XRD was performed on: Dried at 105 degrees</i>	
Silica (Quartz)- SiO ₂	
Iron Oxide (Magnetite) - Fe ₃ O ₄	
Calcium Carbonate (Calcite)-CaCO ₃	
Calcium Fluoride (Fluorite) - CaF ₂	
Amorphous Material	
Possible Compounds..... Sodium Aluminium Silicate (Albite)-NaAlSi₃O₈	
Potassium Aluminium Silicate (Microcline)-KAlSi₃O₈	

Appendix D: XRF and XRD analysis report for scale samples collected from the silencer

Sampling date: 24/02/2020	
Deposit Analysis	
Appearance	
Condition of Solids: Dry	Color of sample: Grey
Solids: Scale	
Elemental Analysis by X-ray Fluorescence	
<i>The sample preparation was: Dried at 105 degrees</i>	
<i>The results are reported as oxides.</i>	
Silica (SiO ₂)	84 wt %
Sodium (Na ₂ O)	4 wt%
Chloride (Cl)	1 wt%
Potassium (K ₂ O)	1 wt%
Sulphur (SO ₃)	1 wt%
Analysis by X-Ray Diffraction	
<i>The XRD was performed on: Dried at 105 degrees</i>	
Amorphous	
Material	
Silica (Silicate) - SiO ₂	
Sodium Chloride (Halite) – NaCl	
Possible Compounds..... Sodium Silicate Hydrate (Magadiite) - Na₂Si₄O₂₉:10H₂O	

Appendix E: XRF and XRD analysis report for scale samples collected from the turbine exhaust

Sampling date: 25/02/2020	
Deposit Analysis	
Appearance	
Color of Sample: Dark Grey	Solids: Scale
Condition of Solids: Dry	
Elemental Analysis by X-ray Fluorescence	
<i>The sample preparation was: Dried at 105 degrees</i>	
<i>The results are reported as oxides.</i>	
Silica (SiO ₂)	52 wt%
Iron (Fe ₂ O ₃)	20 wt%
Sulfur oxide (SO ₃)	10 wt%
Chromium oxide (Cr ₂ O ₃)	1 wt%
Sodium oxide (Na ₂ O)	1wt%
Analysis by X-Ray Diffraction	
<i>The XRD was performed on: Dried at 105 degrees</i>	
Silica (silicate) - SiO ₂	
Iron Oxide (Hematite) - Fe ₂ O ₃	
Iron Oxide(Magnetite) - Fe ₃ O ₄	
Iron Sulfide (Pyrite) -FeS ₂	
Possible Compounds..... Iron	
Silicate	